JOURNAL OF VIROLOGY, Dec. 2006, p. 11833–11851 Vol. 80, No. 23
0022-538X/06/$08.00+0 doi:10.1128/JVI.00857-06

Novel Fiber-Dependent Entry Mechanism for Adenovirus Serotype 5 in Lacrimal Acini[▽]

Jiansong Xie,[1] Lilian Chiang,[1] Janette Contreras,[1] Kaijin Wu,[1] Judy A. Garner,[4] Lali Medina-Kauwe,[5] and Sarah F. Hamm-Alvarez[1,2,3]*

Departments of Pharmacology and Pharmaceutical Sciences,[1] Physiology and Biophysics,[2] Ophthalmology,[3] Cell and Neurobiology,[4] University of Southern California, Los Angeles, and Gene Therapeutics Research Institute, Cedars-Sinai Medical Center, Los Angeles, California[5]

Received 26 April 2006/Accepted 11 September 2006

The established mechanism for infection of most cells with adenovirus serotype 5 (Ad5) involves fiber capsid protein binding to coxsackievirus-adenovirus receptor (CAR) at the cell surface, followed by penton base capsid protein binding to α_v integrins, which triggers clathrin-mediated endocytosis of the virus. Here we determined the identity of the capsid proteins responsible for mediating Ad5 entry into the acinar epithelial cells of the lacrimal gland. Ad5 transduction of primary rabbit lacrimal acinar cells was inhibited by excess Ad5 fiber or knob (terminal region of the fiber) but not excess penton base. Investigation of the interactions of recombinant Ad5 penton base, fiber, and knob with lacrimal acini revealed that the penton base capsid protein remained surface associated, while the knob domain of the fiber capsid protein was rapidly internalized. Introduction of rabbit CAR-specific small interfering RNA (siRNA) into lacrimal acini under conditions that reduced intracellular CAR mRNA significantly inhibited Ad5 transduction, in contrast to a control (nonspecific) siRNA. Preincubation of Ad5 with excess heparin or pretreatment of acini with a heparinase cocktail each inhibited Ad5 transduction by a separate and apparently additive mechanism. Functional and imaging studies revealed that Ad5, fiber, and knob, but not penton base, stimulated macropinocytosis in acini and that inhibition of macropinocytosis significantly reduced Ad5 transduction of acini. However, inhibition of macropinocytosis did not reduce Ad5 uptake. We propose that internalization of Ad5 into lacrimal acini is through a novel fiber-dependent mechanism that includes CAR and heparan sulfate glycosaminoglycans and that the subsequent intracellular trafficking of Ad5 is enhanced by fiber-induced macropinocytosis.

The integrity of the ocular surface is dependent upon maintenance of tear fluid of appropriate composition and volume. There has been considerable interest in the application of gene therapy to the anterior segment of the eye for applications including enhancement of corneal and conjunctival wound healing (9), correction of allograft rejection after corneal transplantation (5), and suppression of lacrimal gland autoimmunity associated with Sjögren's syndrome (61, 62).

Many delivery strategies for introduction of foreign genes into ocular and other tissues have utilized subgroup C adenovirus serotype 5 (Ad5)-derived vectors. The application of traditional Ad5-derived vectors has been limited by host immunogenicity and toxicity. As alternatives, we and others have focused on the use of viral constituents that are able to interact with host factors to facilitate entry of associated DNA. Many next-generation Ad5-derived nonviral vectors use viral capsid proteins to exploit endogenous pathways used by the intact virus for cell entry. The capsid fiber protein has been thought to be responsible for initial cell attachment of Ad5 to the plasma membranes (PM) of many cells, including the well-studied HeLa cell model, through high-affinity binding of its carboxy (C)-terminal globular domain, or "knob" region, to the extracellular N-terminal D1 domain of the coxsackievirus-adenovirus receptor (CAR). This receptor is a ubiquitous integral membrane glycoprotein of the immunoglobulin superfamily which also plays a role in cell adhesion (10, 27, 53). Following the initial attachment, the low-affinity interaction of RGD and LDV motifs exposed in a protruding loop of the penton base with the cell surface integrins is thought to trigger virus uptake by clathrin-dependent receptor-mediated endocytosis. Once internalized, Ad5 is delivered to acidic endosomal compartments and undergoes endosomolysis by escaping to the cytosol upon cell signaling, a process that has been proposed to involve the penton base (42, 43, 57, 58). Ad5 capsid proteins (possibly penton base) then interact with microtubules and dynein/dynactin during transit to the nucleus (31, 36, 60).

In addition to this established internalization pathway in cultured cells, Meier et al. recently demonstrated that Ad2, which is similar to Ad5 in its capsid protein composition, can elicit macropinocytosis in epithelial cells (35). Ad2-induced macropinocytosis could enhance its acid-activated penetration into endosomes even though the virion particles were internalized into clathrin-coated vesicles. Although these and other studies have shed insight into the general mechanisms of Ad internalization, use of cell lines such as HeLa and A549 cells that no longer retain specialized epithelial morphology may not reveal the exact mechanism that Ad5 uses to infect its in vivo target cells, most of which are epithelial in origin.

The acinar epithelial cells of the lacrimal gland (LGAC) are secretory epithelial cells responsible for the basal and stimulated release of a variety of essential proteins into tear fluid

* Corresponding author. Mailing address: Department of Pharmacology and Pharmaceutical Sciences, USC School of Pharmacy, 1985 Zonal Avenue, Los Angeles, CA 90033. Phone: (323) 442-1445. Fax: (323) 442-1390. E-mail: shalvar@hsc.usc.edu.

▽ Published ahead of print on 20 September 2006.

(13, 19, 37, 52). Changes in LGAC secretory functions are associated with diseases ranging in severity from keratoconjunctivitis sicca (dry eye) to the autoimmune disease Sjögren's syndrome (18, 39). Despite real prospects for the rational design of advanced macromolecular therapeutics for treatment of severe dry eye disorders, therapy remains a remote possibility from a drug delivery standpoint. The only methods utilized successfully in animal models for gene delivery to the lacrimal gland have used replication-defective Ad5-derived vectors, which are sufficiently immunogenic to preclude their use in clinical trials (61, 62). To our knowledge, there are no reports regarding delivery of other therapeutic molecules such as proteins, peptides, or antisense oligonucleotides into the lacrimal gland. Ad5 capsid proteins therefore represent promising drug carriers for delivery of macromolecular conjugates to the gland.

We have previously reported that exposure of reconstituted rabbit LGAC to replication-deficient Ad5 at a multiplicity of infection (MOI) of 5 PFU/cell for time intervals as short as 1 to 2 h resulted in transduction of 85 to 90% of acinar cells (30, 50). We have also reported that the recombinant penton base protein of Ad5 appears unable to enter LGAC (25), although it can recapitulate the Ad5 entry pathway in HeLa cells (41). Since Ad5 infects LGAC at high efficiency in an apparently penton-independent manner, we hypothesized that Ad5 might be internalized in LGAC through a unique mechanism. In the studies presented here, as a first step in testing this hypothesis we sought to identify the capsid proteins responsible for mediating Ad5 entry into LGAC. Competition studies showed that fiber, knob, or CAR-specific small interfering RNA (siRNA) significantly and substantially inhibited Ad5 infectivity, while penton base had no effect. Surprisingly, incubation of LGAC with capsid proteins revealed that recombinant penton base protein remained associated with the PM, while recombinant knob was internalized. Inhibition of heparan sulfate-glycosaminoglycan (HS-GAG) interactions by pretreating Ad5 with heparin and by cleavage of cellular HS-GAGs using a heparinase cocktail had a modest but significant additive inhibitory effect on Ad5 infectivity. Analysis of fluorescein isothiocyanate (FITC)-dextran uptake and time-lapse video microscopy of green fluorescent protein (GFP)-actin ruffling showed that Ad5 could stimulate macropinocytosis in LGAC, a process that could also be elicited by fiber and knob but not penton base. Further studies suggested that macropinocytosis is important for efficient Ad5 transduction but that it does not participate directly in Ad5 entry. Altogether, these findings suggest that Ad5 internalization into LGAC is through a unique fiber-dependent pathway that may involve CAR and HS-GAGs rather than the penton base-integrin-mediated endocytotic mechanism seen in other cell models so far investigated.

MATERIALS AND METHODS

Reagents. RGD peptide (Gly-Arg-Gly-Asp-Thr-Pro); LDV peptide (Asp-Glu-Leu-Pro-Gln-Leu-Val-Thr-Leu-Pro-His-Pro-Asn-Leu-His-Gly-Pro-Glu-Ile-Leu-Asp-Val-Pro-Ser-Thr); heparin; heparinase I; heparinase II; heparinase III; chondroitinase ABC; rhodamine-phalloidin; goat anti-rabbit secondary antibody conjugated to FITC; and the protease inhibitors pepstatin A, *N*-tosyl-L-phenylalanine chloromethyl ketone, leupeptin, Nα-*p*-tosyl-L-lysine chloromethyl ketone, Nα-*p*-tosyl-L-arginine methyl ester, and phenylmethylsulfonyl fluoride were purchased from Sigma-Aldrich (St. Louis, Mo.). 5-(*N*-Ethyl-*N*-isopropyl)amiloride (EIPA) was purchased from Alexis Biochemicals (San Diego, Calif.). Latrunculin B (Lat B) was purchased from EMD Biosciences (San Diego, Calif.). Trizol reagent was from Invitrogen Life Technologies (Carlsbad, Calif.). RQ1 RNase-free DNase was from Promega (Madison, Wis.). The QIAquick gel extraction kit was purchased from QIAGEN (Valencia, Calif.). CAR siRNA duplex (sense sequence, 5′-CGCUUCCAUUACGAUAUGA-3′; antisense sequence, 5′-UCAUAUCGUAAUGGAAGCG-3′) and siCONTROL nontargeting siRNA were obtained from Dharmacon RNA Technologies (Lafayette, Colo.). GeneSilencer siRNA transfection reagent was purchased from Gene Therapy Systems (San Diego, Calif.). The Advantage RT-for-PCR kit, the BD SMART RACE (Rapid Amplification of cDNA Ends) cDNA amplification kit, and mouse monoclonal antibody to GFP were purchased from BD Biosciences-Clontech (Palo Alto, Calif.). Rabbit polyclonal antibody to Ad5 was purchased from Access Biomedical (San Diego, Calif.). Rabbit polyclonal antibody to α_v integrin and mouse monoclonal antibody to Ad5 hexon were purchased from Chemicon International (Temecula, Calif.). Mouse monoclonal antibody to Ad5 fiber protein was obtained from Novus Biologicals (Littleton, Colo.). Goat polyclonal antibody to early endosome antigen 1 (EEA1) was from Santa Cruz Biotechnology (Santa Cruz, Calif.), while fluorescein-conjugated horse anti-mouse immunoglobulin G (IgG) was obtained from Vector Laboratories (Burlingame, Calif.). Rhodamine Red-X-conjugated AffiniPure donkey anti-goat IgG was purchased from Jackson ImmunoResearch Laboratories (West Grove, Pa.). Goat anti-rabbit and anti-mouse IRDye 800-conjugated secondary antibodies were purchased from Rockland (Gilbertsville, Pa.). Rabbit polyclonal antibody to rab3D was generated against recombinant mouse rab3D (Antibodies, Inc., Davis, Calif.) and purified using protein A/G Agarose. Matrigel was obtained from Collaborative Biochemicals (Bedford, Mass.). ProLong antifade mounting media and 40,000-molecular weight lysine-fixable fluorescein-conjugated dextran (FITC-dextran) were from Molecular Probes (Eugene, Oreg.). Paraformaldehyde was purchased from Polysciences (Warrington, Pa.). The Russell-Movat pentachrome stain kit was purchased from American Master*Tech Scientific (Lodi, Calif.). Cell culture reagents were obtained from Invitrogen Life Technologies. All other chemicals were reagent grade and were obtained from standard suppliers.

Cell isolation and culture. All animal work was performed in accordance with all institutional guidelines. Female New Zealand White rabbits weighing between 1.8 and 2.2 kg were obtained from Irish Farms (Norco, Calif.). LGAC were isolated and maintained in a laminin-based primary culture system for 2 to 3 days as described previously (12, 22, 24). These culture conditions resulted in reconstitution of polarity, establishment of lumina, and formation of secretory vesicles (11, 12, 22, 24, 29, 30, 49, 54, 55). In some experiments, different cell lines were utilized for comparison to LGAC: these included HeLa cells, Caco-2 cells, CHO cells, and MDCK cells. These cell lines were obtained from ATCC and were split and cultured as recommended.

Generation of recombinant proteins and Ad5 vectors. Recombinant knob, GFP-knob, penton base, and rab3DQL proteins were produced from *Escherichia coli* as His_6-tagged fusion proteins and purified from bacterial lysates using Ni-NTA resin as described previously (25, 32, 33, 34, 41). Recombinant fiber protein and control protein (glutathione-*S*-transferase [GST]) were produced from a baculovirus expression system as described previously (40). The protein contents of purified recombinant proteins were determined using the BCA protein assay (Pierce) with bovine serum albumin as the standard protein. Aliquots of purified proteins were analyzed by sodium dodecyl sulfate-polyacrylamide gel electrophoresis (SDS-PAGE) and verified to be devoid of contaminating species by Coomassie brilliant blue staining. Replication-defective Ad5 containing the GFP reporter gene (Ad-GFP) and replication-defective Ad5 containing the β-galactosidase reporter gene (Ad-LacZ) were constructed, and titers were determined as previously described (50).

Confocal fluorescence microscopy. For detection of Ad5, penton base protein, or knob in fixed cells, reconstituted rabbit LGAC cultured on Matrigel-coated coverslips were incubated with replication-deficient Ad-LacZ (MOI = 5 to 10 PFU/cell), recombinant knob protein (20 μg/ml), or penton base protein (20 μg/ml) for up to 2 h at 4°C (0 min), then warmed to 37°C for various times up to 120 min. After being incubated, the cells were rinsed extensively in ice-cold Dulbecco's phosphate-buffered saline (DPBS) and fixed in 4% paraformaldehyde as previously described (11, 12, 29, 30, 49, 59) prior to the addition of rabbit polyclonal antibody to Ad5 and appropriate secondary fluorophore-conjugated antibodies or fluorescent probes. For analysis of Ad5 recovery in macropinosomes, reconstituted rabbit LGAC cultured on Matrigel-coated coverslips were incubated with replication-deficient Ad-LacZ in binding buffer (Hank's balanced salt solution plus 0.1% bovine serum albumin and 0.02 M HEPES) at 4°C for 1 h. The cells were washed, warmed to 37°C for 5 min, and pulsed with 1 mg/ml FITC-dextran at 37°C for 10 min. The cells were then fixed in 4% paraformaldehyde prior to the addition of mouse monoclonal antibody to Ad5 hexon and appropriate secondary fluorophore-conjugated antibodies or fluores-

cent probes. For colocalization studies with early endosomes, reconstituted rabbit LGAC cultured on Matrigel-coated coverslips were exposed to replication-deficient Ad-LacZ for various times up to 60 min. After being incubated, the cells were fixed in 4% paraformaldehyde prior to the addition of mouse monoclonal antibody to Ad5 hexon, goat polyclonal antibody to EEA1, and appropriate secondary fluorophore-conjugated antibodies or fluorescent probes. Confocal images were obtained with a Zeiss LSM 510 Meta NLO imaging system equipped with argon and red and green HeNe lasers mounted on a vibration-free table. Panels were compiled in Adobe Photoshop 7.0 (Adobe Systems Inc, Mountain View, Calif.).

For live-cell imaging of transduced LGAC expressing GFP-actin, LGAC seeded on Matrigel-coated glass-bottomed round 35-mm dishes (MatTek, Ashland, Mass.) were cotransduced with Ad-tetracycline response element-GFP-actin and Ad-tetracycline transcriptional activator at an MOI of 8 PFU/cell for each for 1 to 2 h before being rinsed and recovered for 18 to 24 h, as previously described (29). These constructs were kindly provided by Dan Kalman, Emory University. The cells were then treated with or without 10 μM Lat B at 37°C for 1 h prior to being incubated with Ad-LacZ (MOI = 100 PFU/cell), recombinant fiber (20 μg/ml), knob (20 μg/ml), or penton base protein (20 μg/ml) in binding buffer at 4°C for 1 h. The cells were washed and warmed to 37°C for 5 min prior to being analyzed by time-lapse confocal fluorescence and differential interference contrast (DIC) microscopy using the Zeiss imaging system mentioned above. Five percent CO_2/95% hydrated air and a temperature of 37°C were maintained in an enclosed chamber during live-cell analysis. Reconstituted acini of a similar size were chosen. GFP fluorescence and DIC images were acquired simultaneously using the 488 line of the argon laser.

For analysis of membrane ruffling under different experimental conditions, data were collected from acinar clusters of comparable cell number and transduction efficiency within a 600-s period representing the period of highest membrane-ruffling activity in each sequence. Each membrane protrusion event occurring within that time frame was recorded at its largest diameter, using the LSM Image Browser overlay tool. These values were then divided into diameter ranges. The number of ruffling events in each range was classified by treatment group and divided by the number of sequences analyzed to obtain an average value per sequence for each treatment.

FITC-dextran uptake assay. For FITC-dextran uptake, resuspended LGAC pretreated with dimethyl sulfoxide (DMSO), 500 μM EIPA, or 10 μM Lat B at 37°C for 1 h were incubated with Ad-LacZ (MOI = 100 PFU/cell), recombinant fiber (20 μg/ml), knob (20 μg/ml), or penton base protein (20 μg/ml) in binding buffer at 4°C for 1 h. The cells were washed, warmed to 37°C for 5 min, and pulsed with 1 mg/ml FITC-dextran (40 kDa; Molecular Probes) at 37°C for 10 min. Dextran uptake was stopped by washing in ice-cold DPBS, and surface-bound dextran was stripped off in 0.1 M sodium acetate–0.05 M NaCl (pH 5.5) at 4°C for 10 min (35). The cells were washed in cold DPBS, and FITC-dextran uptake was measured by flow cytometry.

Cell-binding assay. To assess surface binding, control rabbit LGAC or HeLa cells treated with or without recombinant penton or GFP-knob protein (20 μg/ml) for 0 min and 60 min were then exposed to 0.2 mg/ml trypsin-EDTA at 4°C for 1 h (23). The cells were lysed in radioimmunoprecipitation (RIPA) buffer by 15 passages through a 23-gauge syringe needle followed by two freeze-thaw cycles. The lysate was centrifuged for 5 min at 3,000 rpm in an Eppendorf 5415C centrifuge at 4°C, and the supernatant was collected. The cell lysates (150 μg) were blotted with appropriate primary antibodies (rabbit polyclonal anti-Ad5 antibody for penton detection and mouse monoclonal anti-GFP antibody for GFP-knob detection) and IRDye 800-conjugated secondary antibodies. A similar protocol was used to evaluate Ad5 uptake (15 PFU/cell) in LGAC pretreated with either 500 μM EIPA or 10 μM Lat B at 37°C for 1 h relative to that for LGAC pretreated with vehicle (DMSO); fiber protein internalization in cell lysates was tracked using the mouse monoclonal anti-fiber protein antibody for fiber detection in combination with an appropriate IRDye 800-conjugated secondary antibody.

Cell infection assays. Relative transduction efficiencies for rabbit LGAC, MDCK, Caco-2, CHO, and HeLa cells were determined by adding Ad-GFP at an MOI of 5 or 10 PFU/cell, incubating the cells for 1 h at 4°C before washing them, and then incubating the cells for 10 to 12 h at 37°C. GFP positivity was determined by flow cytometry as previously described (50). To compare the abilities of individual viral components to block Ad5 transduction of LGAC and HeLa cells, the cells were preincubated with various doses of recombinant penton, fiber, knob, or the penton-blocking peptides RGD and LDV in binding buffer for 2 h at 4°C. Replication-deficient Ad-GFP was then added at an MOI of 2 PFU/cell, and the cells were incubated for 1 h at 4°C before being washed and incubated for 10 to 12 h at 37°C. The amount of cell-bound virus was indirectly assayed by GFP positivity, determined by flow cytometry as described previously (50). In some experiments, Ad-GFP was preincubated with heparin at 37°C for 1 h before being added to the cells. In other experiments, freshly isolated LGAC were seeded on Matrigel-coated 12-well plates for 3 h to allow adherence, then treated with 10 U/ml heparinase cocktail (mixture of heparinases I, I, and III, each at 10 U/ml) or chondroitinase ABC in PBS containing 1 mM $CaCl_2$, 0.5 mM $MgCl_2$, 1 mg/ml glucose, 1% fetal bovine serum, and the protease inhibitors phenylmethylsulfonyl fluoride (100 μM) and leupeptin (20 μM) for 2 h at 37°C (15). After this treatment, the cells were rinsed well in Hank's balanced salt solution, resuspended in binding buffer, and incubated with Ad-GFP as described above.

Rabbit CAR cDNA cloning by reverse transcription-PCR (RT-PCR). Total RNA was isolated from HeLa cells and mouse or rabbit LGAC using Trizol reagent. RNA samples were treated by RQ1 RNase-free DNase, and cDNA was then synthesized using the Advantage RT-for-PCR kit according to the manufacturer's instructions. CAR gene expression was analyzed by PCR using a primer designed according to a sequence conserved in human and mouse CAR (5′ end starting from human CAR sequence F5275, GTTCTTGTTAAGCCTT CAGGT; 3′ end starting from human CAR sequence R963, GCACATCTTCC CTGATATC). PCR products of ~400 base pairs (bp) were extracted using a QIAquick gel extraction kit according to the manufacturer's instructions and subjected to DNA sequencing analysis, resulting in a 357-bp reliable rabbit CAR sequence. To obtain additional sequences of rabbit acinar CAR, the BD SMART RACE cDNA amplification kit was used for cDNA synthesis according to the manufacturer's instructions. The 5′ fragment of rabbit CAR was produced by RACE PCR using the specially designed 5′-end RACE primer and CAR-specific downstream primer designed according to the 357-bp reliable sequence (GGT CCCAGAGTACTCAGAAGTGGC). The 3′ fragment of rabbit CAR was generated by RACE PCR using a CAR-specific upstream primer (TGCCCGACTCA TGGTTACCAGAAATG) and modified oligo(T). 5′- and 3′-RACE fragments of CAR were extracted and subjected to DNA sequencing analysis, resulting in generation of the entire rabbit CAR coding region of a 1,098-bp sequence.

Analysis of CAR mRNA in tissue by real-time PCR. For analysis of CAR expression in rabbit tissues, total RNAs were prepared from liver, lacrimal gland, and spleen from each of two rabbits, using the VERSAGENE RNA Tissue kit (Gentra Systems, Minneapolis, Minn.). Reverse transcription was conducted with an Advantage RT-for-PCR kit (Clontech, Mountain View, Calif.), and real-time PCR was conducted in a 7900 HT system (Applied Biosystems, Foster City, Calif.). Hypoxanthine phosphoribosyl transferase 1 (HPRT1) and phosphoglycerate kinase 1 (PGK1) were selected as endogenous controls. HPRT1 primers consisted of F-301 (5′-AGACTGAAGAGCTACTGTAATGA-3′) and R-397 (5′-CAATCAAGACATTCTTTCCAGTTAAG-3′). PGK1 primers consisted of F-402 (TGCTTCTGGGAACAAGGTTAAA-3′) and R-512 (5′-CGG TGAGCAGTGCCAAA-3′). Two pairs of CAR primers were used for the assay. The first primer pair consisted of F15 (5′-GCGCTTCGTACTCCTGTGC-3′) and R-101 (5′-CCTTTGGCTTTTTCAATCATCTG-3′). The second primer pair consisted of F-496 (5′-GAAGGTTCGC-TTCCATTACGA-3′) and R-593 (5′-GATATAACAGGTGAAGTCATTTCTGG-3′). All the primers were positioned by assigning the A of the first ATG in the CAR cDNA as number 1. Each reaction was conducted in triplicate, and the results were averaged. SYBR green was used as a detection dye.

siRNA knockdown of CAR. The 1,098-bp rabbit CAR sequence was screened using Dharmacon's online designer for siRNA generation. The resulting CAR siRNA duplex (sense sequence, 5′-CGCUUCCAUUACGAUAUGA-3′; antisense sequence, 5′-UCAUAUCGUAAUGGAAGCG-3′) was generated by Dharmacon and applied to LGAC seeded at 2×10^6 cells/ml on day 1 of the culture (100 nM) using the GeneSilencer siRNA transfection reagent. A siCONTROL nontargeting siRNA from Dharmacon was used in parallel to control for non-sequence-specific effects. Blast analysis confirmed that the siCONTROL has at least four mismatches with all known mammalian genes. LGAC were cultured for 48 h after introduction of siRNA and assessed for CAR mRNA knockdown by RT-PCR as described above or for the effect of silencing CAR-expression on Ad-GFP transduction efficiency by flow cytometry. Finally, the CAR mRNA knockdown suggested by RT-PCR was verified using real-time PCR. Briefly, total RNA was prepared from the CAR siRNA-treated and control LGAC at 48 h, and 1 μg of total RNA from each sample was used for reverse transcription in a 20-μl aliquot. Real-time PCR, conducted with a 7900 HT Fast real-time PCR system, utilized conditions of 95°C for 10 min and 95°C for 15 s, followed by 40 cycles at 60°C for 1 min. Two pairs of CAR primers were used for quantification, as described in the preceding section. PGK1 was selected as the endogenous control. One microliter of RT product was used as a template in each 10 μl of CAR PCR, and 1/10 μl of RT product was used in each 10 μl of PGK1 PCR. Each treatment was done in triplicate, and SYBR green was used as the detection dye. For estimation of transfection efficiencies, BLOCK-iT Fluorescent Oligo (Invitrogen Life Technologies, Carlsbad, Calif.) was substituted for

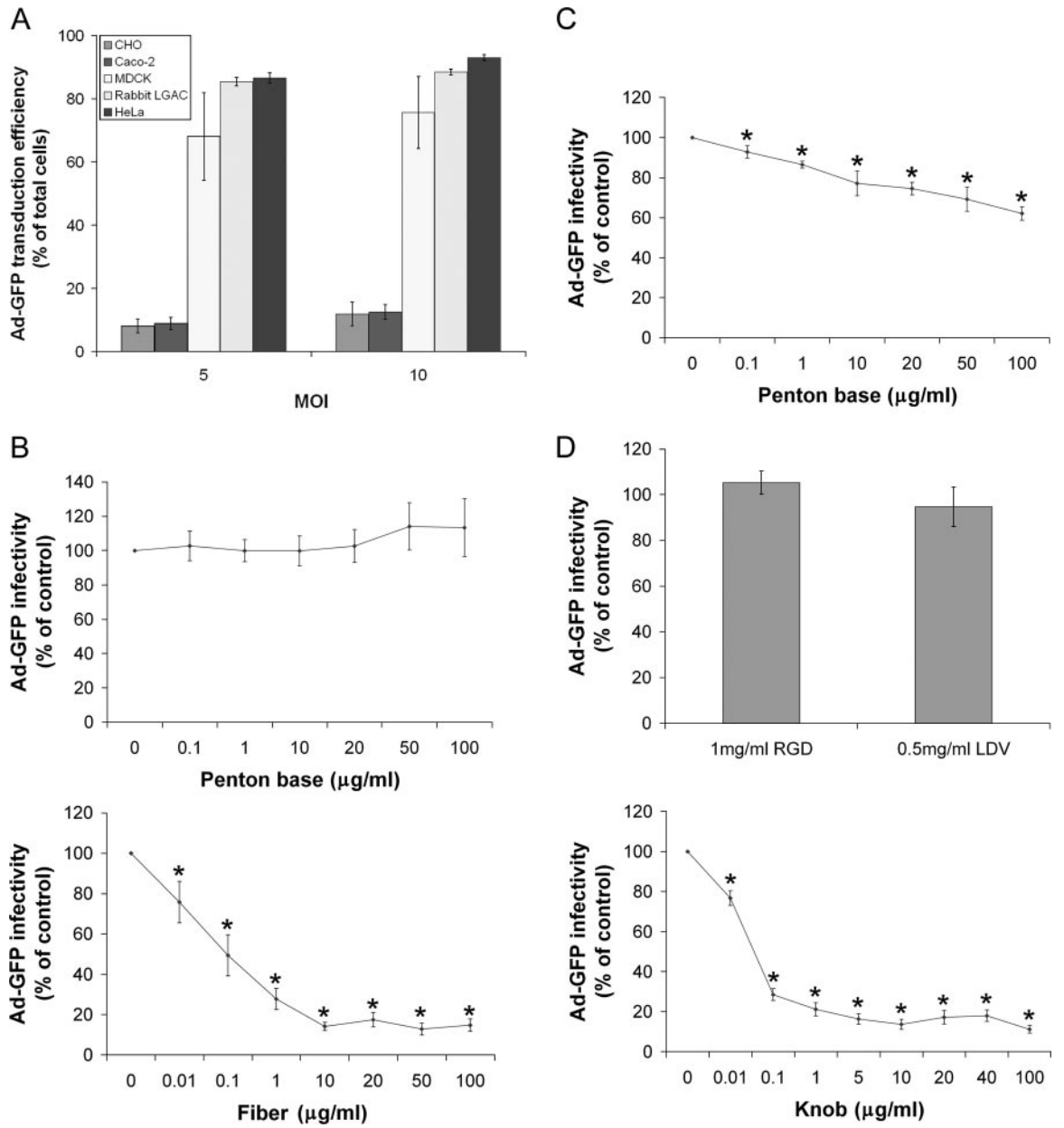

FIG. 1. Ad5 transduction efficiency in LGAC and sensitivity to penton base, fiber, and knob protein. (A) The percentage of transduction efficiency of Ad-GFP in rabbit LGAC is approximately equivalent to that in HeLa cells, significantly higher than that in MDCK cells, and eight- to ninefold higher than that in CHO cells and Caco-2 cells. Rabbit LGAC were seeded onto Matrigel-coated 12-well plates at 2×10^6 cells/well and used on day 2, while other cell lines were seeded onto noncoated 12-well plates at 1×10^5 cells/well and used at 80% confluence. Ad-GFP was then added at an MOI of 2 PFU/cell, and the cells were incubated for 1 h at 4°C, washed, and then incubated for 10 to 12 h at 37°C. GFP positivity was determined by flow cytometry ($n = 5$). (B) Preincubation of LGAC with fiber substantially lowers Ad-GFP infectivity, while preincubation with penton base appears to have little effect (for penton base experiments, $n = 7$; for fiber experiments, $n = 4$). (C) Preincubation of HeLa cells with penton base results in reduced Ad-GFP infectivity ($n = 5$). (D) Preincubation of LGAC with knob substantially reduced Ad-GFP transduction efficiency, while preincubation with RGD and LDV had little effect (for RGD, $n = 3$; for LDV, $n = 4$; and for knob, $n = 8$). For the experiments for panels B to D, rabbit LGAC were seeded onto Matrigel-coated 12-well plates at 2×10^6 cells/well and HeLa cells were seeded onto uncoated 12-well plates at 1×10^5 cells/well. On day 2 of the culture (80% confluence for HeLa cells), the cells were preincubated with the indicated concentrations of recombinant knob, fiber, penton base, or the penton base-blocking peptides RGD or LDV for 2 h at 4°C. Ad-GFP was then added at an MOI of 2 PFU/cell, and the cells were incubated for 1 h at 4°C, washed, and incubated for 10 to 12 h at 37°C. GFP positivity was determined by flow cytometry. In all panels, * indicates significance at a P value of ≤ 0.05, based on results for the control. Error bars represent the standard error of the mean (SEM).

the siRNAs under the conditions described above. The transfection efficiencies of LGAC were assessed between 6 and 24 h posttransfection using fluorescence microscopy.

Nucleotide sequence accession number. The entire coding sequence of rabbit lacrimal acinar CAR has been deposited in GenBank under accession number EF034116.

RESULTS

Ad5 transduction into LGAC is inhibited by fiber but not penton base. Previous studies utilizing replication-defective Ad5 to promote exogenous gene expression in LGAC sug-

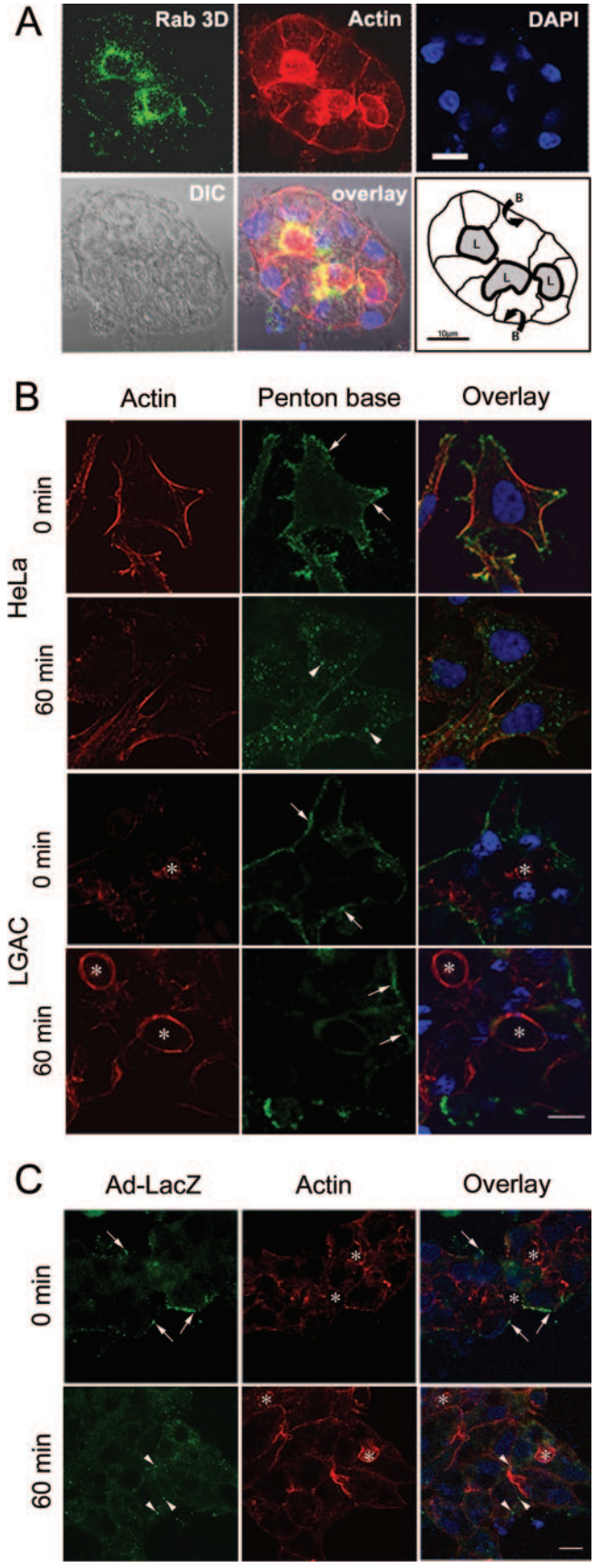

gested that these cells were transduced by Ad5 with high efficiency (29, 30, 50). To confirm this, we compared the transduction of LGAC to that of several commonly utilized cell lines, including CHO cells, Caco-2 cells, MDCK cells, and HeLa cells. HeLa cells are considered the gold standard for Ad5 infection, exhibiting a very high transduction efficiency. As shown in Fig. 1A, the transduction efficiency of LGAC by Ad5 at an equivalent MOI was comparable to that for HeLa cells, slightly higher than for MDCK cells, and substantially higher than for CHO and Caco-2 cells.

Since early events involving interactions between Ad5 and its cell surface receptors play an essential role in determining Ad5 vector tropism, it was important to identify the capsid proteins responsible for mediating Ad5 entry into LGAC. To address this question, a series of competition studies which measured replication-deficient Ad-GFP infectivity under different experimental conditions were performed using flow cytometry. Since Ad5 entry into most cells involves interaction of fiber and penton base proteins sequentially with CAR and integrins, respectively, we first assessed transduction efficiency with Ad-GFP in the presence of various amounts of these recombinant proteins. As shown in Fig. 1B, at concentrations of up to 100 μg/ml of penton base, we found no inhibition of Ad5 transduction into LGAC. Exposure of HeLa cells to penton base protein elicited a significant inhibition of Ad5 transduction at doses as low as 0.1 μg/ml, while the extent of the inhibition increased with increasing concentrations of penton, up to 40% at 100 μg/ml (Fig. 1C).

To verify the apparent differences in the interactions of the penton base protein with HeLa cells and LGAC, we utilized confocal fluorescence microscopy to assess the locations of penton base protein in the cells at different time intervals. Individual LGAC cells reassociate in culture to form acinus-like structures organized around the lumen, the secretory domain that is bounded by the apical membranes of adjacent acinar cells. The nuclei are localized towards the basolateral membranes. Our previous work has established that actin filaments form a dense subapical meshwork beneath the apical

FIG. 2. LGAC morphology and uptake of Ad5 and penton base protein. (A) The intracellular components of a reconstituted rabbit lacrimal gland acinus. Cells were triple stained with antibodies to Rab 3D (green), actin (red), or DAPI (4′,6′-diamidino-2-phenylindole) (blue) to show the localization of mature secretory vesicles, actin filaments, and nuclei, respectively. The diagram shows the location of lumina (L) bounded by the apical PM of epithelial cells (dark line). Basolateral membranes (B) of the epithelial cells are indicated by arrows. (B) Penton base uptake in HeLa and LGAC. HeLa cells or LGAC were seeded onto uncoated or Matrigel-coated 12-well plates at 1×10^5 cells/well or 2×10^6 cells/well, respectively. On day 2 (HeLa) or day 3 (LGAC) of the culture, control cells or cells exposed to penton base (20 μg/ml) for 0 min and 60 min at 37°C were fixed and processed to fluorescence label penton base (green), actin filaments (red), and nuclei (blue). Arrows, association of penton base with PM; arrowheads, penton base in perinuclear region. (C) Control rabbit LGAC or LGAC exposed to replication-deficient Ad-LacZ (MOI = 5) for 0 min and 60 min were fixed and processed to fluorescence label Ad5 proteins (green), actin filaments (red), and nuclei (blue). Arrows, association of Ad5 with basolateral membranes; arrowheads, accumulation of Ad5 in intracellular compartments; bar, 10 μm; *, apical/luminal region.

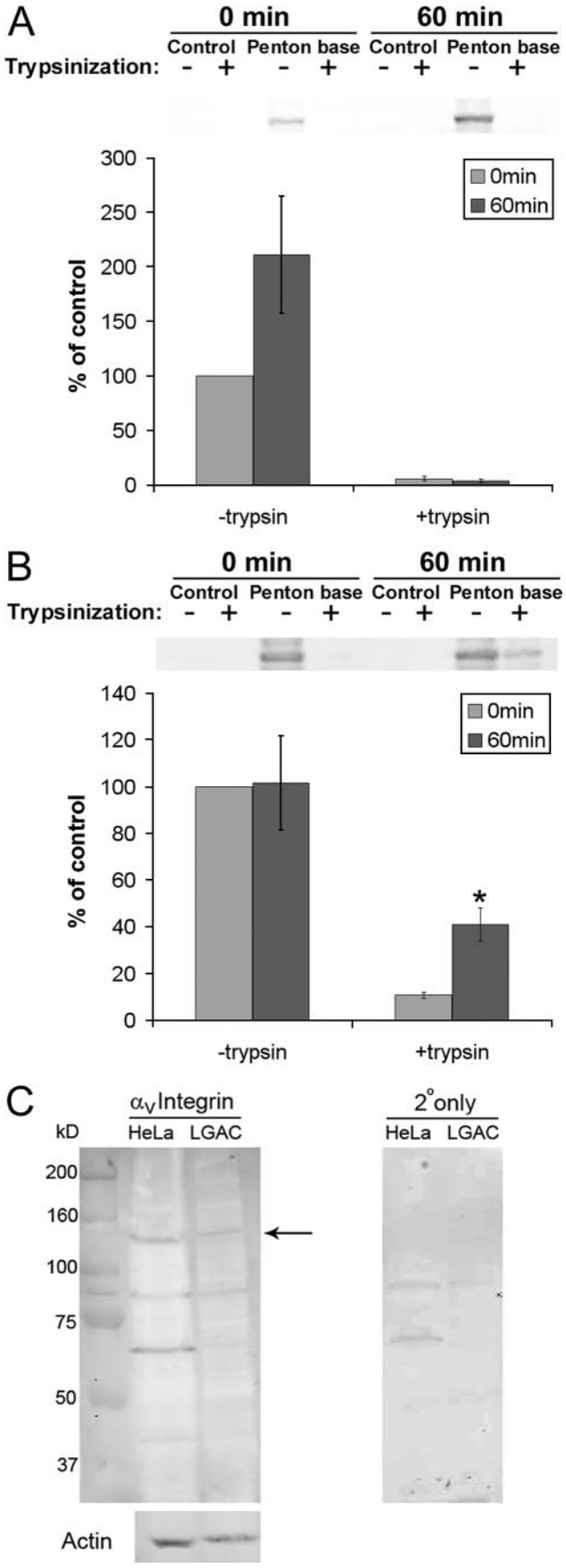

PM which separates mature secretory vesicles from the site of regulated secretion until cell stimulation occurs (12, 29). Thus, this characteristic accumulation of actin filaments can be used to identify the apical PM in these cultures. In Fig. 2A, a typical reconstituted acinus comprised of LGAC is shown with several reference points, including mature secretory vesicles labeled with antibodies to rab3D, actin filaments, nuclei, and the DIC image. The schematic diagram shows the organization of the lumina bounded by the apical PM of adjacent cells and the positions of the basolateral membranes (Fig. 2A) within this cluster.

Uptake experiments analyzed by confocal fluorescence microscopy showed that after 60 min, much of the membrane-associated penton base protein in HeLa cells had accumulated in the perinuclear region (Fig. 2B); we have previously shown that this pattern of accumulation in HeLa cells is intracellular (41). This incubation time course was also sufficient for internalization of intact Ad5 in LGAC (Fig. 2C); in contrast, under these conditions, the penton base protein remained associated with the PM and intercellular junctions in LGAC (Fig. 2B). Addition of recombinant fiber did not confer internalization to penton in this assay (data not shown). As additional confirmation of penton-independent transduction, molar excesses (200 to 500) of RGD or LDV peptides, which should compete for penton binding to the RGD and LDV motifs in surface integrins, had no effect on Ad5 transduction into LGAC (Fig. 1D). By confirming that the penton base behaved as previously reported in HeLa cells (41), these studies verified the efficacy of our recombinant penton base protein.

We also explored the contribution of the fiber protein to Ad5 transduction into LGAC. Fiber protein at doses as low as 10 ng/ml significantly ($P \leq 0.05$) inhibited Ad5 transduction, reaching a maximum of 80% inhibition at 10 μg/ml of fiber protein (Fig. 1B). Fiber protein was not toxic to LGAC; trypan

FIG. 3. Penton base remains surface bound in LGAC. (A) Penton base is vulnerable to trypsin at 60 min after exposure in LGAC. Rabbit LGAC were seeded onto Matrigel-coated 12-well plates at 2×10^6 cells/well. On day 2 of the culture, LGAC with or without exposure to penton base protein (20 μg/ml) for 0 min or 60 min at 37°C were treated with 0.2 mg/ml trypsin-EDTA for 1 h at 4°C or not treated and were lysed, using RIPA buffer. Cell lysates (150 μg/lane) were blotted with polyclonal antibody to Ad5 proteins and IRDye800-conjugated secondary antibody. Data were normalized in each preparation to that for penton base association at 0 min minus that for trypsin. Error bars represent SEM ($n = 3$). (B) Penton base acquires trypsin resistance after incubation in HeLa cells. HeLa cells were seeded on 12-well plates. When they reached 80% confluence, they were exposed to penton base protein (10 to 50 μg/ml) for 0 or 60 min at 37°C or not exposed and then were treated with trypsin-EDTA or not treated and were processed as described above. Data for each preparation were normalized to that for penton base association at 0 min minus that for trypsin. *, significant at $P \leq 0.05$ based on results for cells at 0 min. Error bars represent SEM ($n = 5$). (C) LGAC express α_v integrins. Western blots of α_v integrin expression in rabbit LGAC and HeLa cells are shown. LGAC and HeLa cell lysates prepared using RIPA buffer (150 μg/lane) were blotted with a rabbit polyclonal antibody to α_v integrin and IRDye 800-conjugated secondary antibody. The arrow depicts a band at 150 kDa, the reported molecular mass of the protein. The same lanes, reprobed for actin content, are shown below, while the signal associated with the secondary antibody (2^o) alone is shown in the panel to the right.

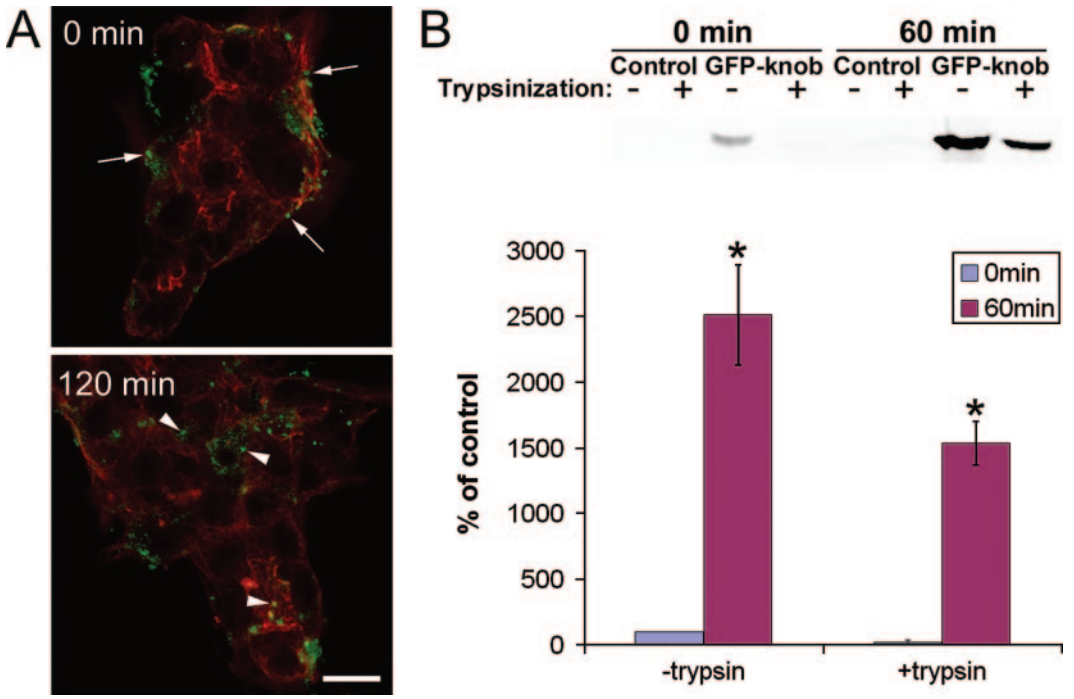

FIG. 4. Knob internalization in LGAC. (A) Knob protein internalized in LGAC as determined by immunofluorescence tagging. Rabbit LGAC were seeded onto Matrigel-coated 12-well plates at 2×10^6 cells/well. On day 3 of the culture, control rabbit LGAC or LGAC exposed to knob protein (20 μg/ml) for 0 min and 120 min at 37°C were fixed and processed to fluorescence label knob (green) and actin filaments (red). Arrows, association of knob with basolateral PM; arrowheads, accumulation of knob in intracellular compartments; bar, 10 μm. (B) Knob protein acquired trypsin resistance after 60 min of incubation with LGAC. Rabbit LGAC were seeded in 150-mm petri dishes at a density of 2×10^6 cells/ml. On day 2 of the culture, LGAC exposed to GFP-knob protein (20 μg/ml) for 0 min or 60 min were treated with 0.2 mg/ml trypsin-EDTA for 1 h at 4°C and lysed using RIPA buffer. Cell lysates (150 μg/lane) were blotted with monoclonal antibody to GFP and IRDye800-conjugated secondary antibody. The data for each preparation were normalized to that for GFP-knob association at 0 min minus that for trypsin ($n = 3$). *, significant at $P \leq 0.05$ based on results for cells at 0 min. Error bars represent the SEM.

blue exclusion studies verified that fiber protein exposure at 20 μg/ml for 2 h was associated with cell viability that was 97 ± 1% of that of untreated LGAC ($n = 4$). We also found that knob, the terminal domain of the fiber protein which becomes a trimer in solution (34), elicited a potent inhibitory effect on Ad5 infectivity comparable to that of the fiber (Fig. 1D). Preliminary data from primary-cultured rat acinar cells showed evidence for the same fiber-dependent, penton-independent Ad5 uptake as for the rabbit (data not shown), suggesting that this uptake mechanism in the lacrimal gland is conserved across species.

Penton base protein is not internalized in LGAC. Results from the experiments shown in Fig. 1 and 2 suggested that penton base protein might not enter LGAC efficiently, in contrast to its behavior in HeLa cells. To confirm this, we used a trypsinization-based biochemical assay to measure the amount of penton base associated with the cell surface versus intracellular membranes and cytosol. For this assay, the amount of penton base associated with each cell type at 0 min in the absence of trypsin represents the control value. As shown in Fig. 3A, penton associated with LGAC for either 0 or 60 min exhibited a similar sensitivity to trypsin, which resulted in cleavage of almost all associated penton base protein. This response is consistent with a lack of internalization of penton base protein in LGAC. However, much of the penton base associated with HeLa cells after 60 min of incubation at 37°C exhibited trypsin resistance, indicative of internalization (Fig. 3B). These biochemical studies confirmed the findings shown in Fig. 1 and 2, suggesting that penton base is not readily internalized in LGAC. This observation for LGAC was quite surprising, since penton base readily accumulates in intracellular compartments in other cells, including HeLa cells (Fig. 2B) (28, 41), and is thought to be able to mimic the entire Ad entry pathway in these cells. Furthermore, Western blotting confirmed that α_v integrin, the major receptor for the penton base, is expressed in LGAC at levels comparable to those for HeLa cells (Fig. 3C), consistent with a previous study reporting the expression of α_v integrin in intact lacrimal tissue (21).

Knob is internalized in LGAC. Incubation of LGAC with recombinant knob protein showed, surprisingly, just the opposite result to that of the penton base protein. While knob protein was surface associated at 0 min, its detection by immunofluorescence in a series of punctate spots located deep within the acini at 60 min was consistent with its internalization in LGAC (Fig. 4A). This labeling pattern was also reminiscent of the internalization pattern for Ad5 in LGAC (Fig. 2C). This apparent internalization in acinar cells was quite distinct from our findings for HeLa cells, showing that the same Ad5 knob remains associated with surface-bound CAR (40). Trypsinization assays verified the findings by confocal fluorescence microscopy. In this assay, the amount of cell-associated knob protein at 0 min in the absence of trypsin represents the

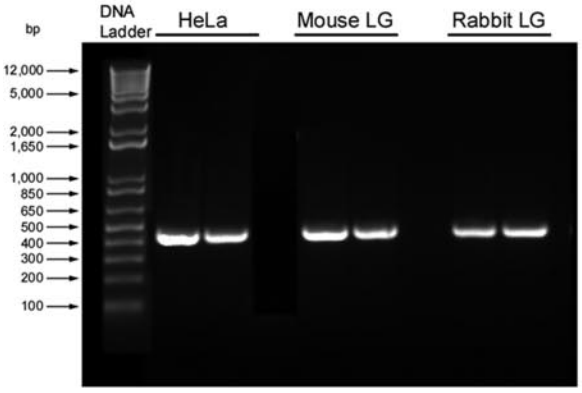

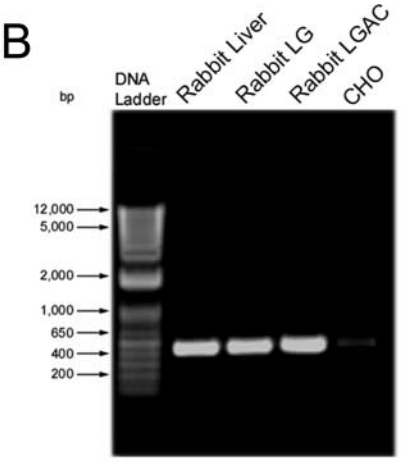

C

```
                5'
Rabbit    1  ATGGCGCTTCTGCTGCGCTTCGTACTCCTGTGCGGCGTCGCGGATTTCGCCAGAAGTTTG   60
Human     1  ...........C......T.......G..........A..A.T.................   60
Mouse     1  ...GC..A...T.......G...T.......GA..........A....TG.....     60

Rabbit   61  ACTATCATTAATCCTGAACAGATGATTGAAAAAGCCAAAGGGGAAACTGCCTATCTACCA  120
Human    61  .G.....C..C.......G.....................................G...  120
Mouse    61  .GC....C..CA..C.......G...C.....................G.........  120

Rabbit  121  TGCAAATTTACTGTTAGTGACGAAGACCAGGGACCACTGGACATTGAGTGGCTACTATCA  180
Human   121  ...........GC.....CC..............G........C........GA.....  180
Mouse   121  .....G......C.C...CC.....................................C  180

Rabbit  181  CCAGCTGATAATCAGAAGCCGGATCAAGTGATTATTTTATATTCTGGAGACAAAATTTAT  240
Human   181  ..................GT.....................................  240
Mouse   181  ..GT.......C....TAGT............C.....G.....................  240

Rabbit  241  GTTGACTACTATCAAGATCTGAAAGGACGAGTACATTTTACAAGCAATGATATCACATCT  300
Human   241  .A..........C.............C.............G..T......C...A....  300
Mouse   241  .A.A.........CG.............G...........G..T..C...G...AG...  300

Rabbit  301  GGTGATGCATCAATAAATGTAACAAATTTACAGTTATCGGATATCGGCATTTATCAGTGT  360
Human   301  .....................G........AC.G..A.....T....CA.........C  360
Mouse   301  ..C..C.....T........G..C..CC.G...C.G.....C..T....C...C.....C  360

Rabbit  361  AAAGTGAAAAAAGCTCCTGGTGTTGCAAATAAGAAAGTTCAACTTACAGTTCTTGTTAAG  420
Human   361  ....................................GA....T..GGT.............  420
Mouse   361  ........G.....C.....G..............T.C.TG..G..C.............  420

Rabbit  421  CCTTCAGGTATAAGATGCTTCATTGATGGGTCAGAAGAAATTGGAAATGACTTTAAACTA  480
Human   421  .........GCG.....T.A.G.......A..T.............G.........GA..  480
Mouse   421  .........C..........G.G.....A..G.....G..............C..G...  480

Rabbit  481  AAATGCGAACCCAAAGAAGGTTCGCTTCCATTACGATATGAATGGCAAAAACTGTCTGAC  540
Human   481  .....T.....A..........A.........AG.....G.........T........  540
Mouse   481  .....T........G.....C..C......C...AG.T.........G........G...  540

Rabbit  541  TCTCAGAAAATGCCCGACTCATGGTTACCAGAAATGACTTCACCTGTTATATCTGTAAAA  600
Human   541  ..A............ACT.........G..............T.................  600
Mouse   541  ..C....C......TACGC.....C.GG..........G.....A...........G..G  600

Rabbit  601  AATGCCACTTCTGAGTACTCTGGGACCTATAGTTGTACAGTCAGAAACCGGGTGGGCTCC  660
Human   601  ......T.....................A..C..C..............A.A........T  660
Mouse   601  ..C....G.........T........A..C..C..C..G..TCA....A.A........T  660

Rabbit  661  GATCAGTGTCTGCTGCGCCTAGATGTTGTTCCTCCTTCAAATAGAGCTGGAACAATTGCA  720
Human   661  ........C...T....T...A.C.....C.............A.........CT.....  720
Mouse   661  ..C......A.......A.....C.....C..A..C..C..CC....C.....G..C..G  720

Rabbit  721  GGAGCTATTATAGGAACTTTGCTTGCTCTAGTGCTCATTGGTTGTATCGTCTTTTGCTGT  780
Human   721  .....C..........................C...........CT....A..........  780
Mouse   721  ..C..CG.C.....G..GC....G..C..T.........C..GGCC...C.....C.....  780

Rabbit  781  CATAAAAAGCGCAGAGAAGAAAAATATGAAAAGGAAGTTCATCATGACATCAGGGAAGAT  840
Human   781  .G..........................................C..T.............  840
Mouse   781  ..C.GG..A...........G..G..C..G.................T.............  840

Rabbit  841  GTGCCTCCTCCCAAGAGTCGTACCTCTACTGCCAGAAGCTACATTGGCAGCAATCATTCA  900
Human   841  .....A.....A.....C.....G..C.................C.....T........  900
Mouse   841  ..........A........G..A..C........G.....T...........C.....C  900

Rabbit  901  TCCCTGGGATCCATGTCCCCTTCTAACATGGAAGGGTACTCCAAGACTCTGTATAACCAA  960
Human   901  ........G........T.....C...........A..T..........A..........  960
Mouse   901  ....................C...........G.....T........G.A..........  960

Rabbit  961  GTCCCAAGTGAAGACTTTGAACGTGCTCCTCAGAGTCCAACTCTCCCACCTGCTAAGGTA 1020
Human   961  ..A.....................CA.............G.....................  1020
Mouse   961  .....C.....................G........C..G.....GG....C........  1020

Rabbit 1021  GCTGCCCCTAATCTAAGTCGAATGGGCGCTGTTCCTGTGATGATTCCAGCACAGAGCAAG 1080
Human  1021  ........................T..GA.....................................  1080
Mouse  1021  ..............C...........A..G.....................T.............  1080

Rabbit 1081  GATGGGTCCATAGTATAG  1098
Human  1081  ........T......|...  1098
Mouse  1081  ..C.....T......|...  1098
                          3'
```

```
                N
Rabbit    1  MALLLRFVLLCGVADFARSLTIINPEQMIEKAKGETAYLPCKFTVSDEDQGPLDIEWLLS   60
Human     1  .....C.......V......S.TT..E..................L.P...........I.   60
Mouse     1  ..R..C......I...TSG.S.TT...R................L.P...........I.   60

Rabbit   61  PADNQKPDQVIILYSGDKIYVDYYQDLKGRVHFTSNDITSGDASINVTNLQLSDIGIYQC  120
Human    61  ......V.............D...P.............LK..................T...  120
Mouse    61  .S...IV.............DN..P.............VK..................T...  120

Rabbit  121  KVKKAPGVANKKVQLTVLVKPSGIRCFIDGSEEIGNDFKLKCEPKEGSLPLRYEWQKLSD  180
Human   121  ............IM.V.......A..YV.......S...I............Q........  180
Mouse   121  ............FL.........T...V.......................QF.......  180

Rabbit  181  SQKMPDSWLPEMTSPVISVKNATSEYSGTYSCTVRNRVGSDQCLLRLDVVPPSNRAGTIA  240
Human   181  .....T...A....S.......S.........................N......K..L..  240
Mouse   181  ..T..TP..A............S...........Q........M.............|...  240

Rabbit  241  GAIIGTLLALVLIGCIVFCCHkkrreekyekeVHHDIREDVPPPKSRTSTARSYIGSNHS  300
Human   241  ..........A...L.I...R.....................................  300
Mouse   241  ..V...........A.L....R.....................................  300

Rabbit  301  SLGSMSPSNMEGYSKTLYNQVPSEDFERAPQSPTLPPAKVAAPNLSRMGAVPVMIPAQSK  360
Human   301  ................Q..........T.....................I.........  360
Mouse   301  ................Q.................A.....................  360

Rabbit  361  DGSIV  365
Human   361  .....  365
Mouse   361  .....  365
                C
```

control value. In contrast to the results obtained with penton base, acute exposure of LGAC to knob resulted in its rapid acquisition of trypsin resistance, indicative of internalization (Fig. 4B).

CAR expression in LGAC. The studies described above suggested a fiber-dependent entry mechanism for Ad5 in LGAC and further suggested the ability of knob (and, by extension, fiber) to readily enter LGAC. An obvious candidate for fiber binding is CAR. We used two commercial antibodies generated against human CAR to assess the expression and distribution of CAR in LGAC, but they failed to recognize the major CAR isoform at 46 kDa in LGAC extracts (data not shown). Using primers designed from a sequence conserved in human and mouse CAR, we evaluated CAR expression in rabbit lacrimal gland by RT-PCR. As shown in Fig. 5A, both rabbit and mouse lacrimal glands expressed CAR. These primers provided only a weak signal with RNA from CHO cells, which lack significant CAR expression (4), under the same conditions as those associated with production of a significant signal from rabbit tissues (Fig. 5B). Amplification of the rabbit lacrimal acinar CAR sequence by RACE PCR yielded a reliable 1,098-bp sequence. Alignment of this sequence with the known sequences of mouse and human CAR confirmed its identity as a full-length coding sequence of the rabbit orthologue (Fig. 5C). The rabbit CAR sequence showed 89% and 83% sequence identity with human and mouse CAR, respectively. Also, as shown in Fig. 5C, the predicted protein sequences were highly homologous, indicating 89% amino acid homology with human CAR and 88% homology with mouse CAR.

We also evaluated the relative expression levels of CAR in rabbit tissues from the spleen, liver, and lacrimal gland using real time PCR. Liver expresses very high levels of CAR in contrast to spleen, according to a previous report (17). Levels of CAR in lacrimal gland were almost as high as those in liver (~70% of the values for liver) and were considerably higher than those in spleen (~30 to 100 times higher) (Table 1). This finding indicates a very high expression level of CAR in the lacrimal gland.

Functional role of CAR in Ad5 transduction. If CAR participates in virus attachment and/or internalization, then inhibition of its expression or function in LGAC should inhibit Ad5 transduction relative to that in untreated acinar cells. siRNA is an effective tool for inhibiting gene expression in mammalian cells (6, 16, 44). The availability of the complete rabbit LGAC CAR coding sequence enabled us to design siRNAs for knockdown of rabbit CAR in LGAC. Figure 6A shows the results of semiquantitative RT-PCRs and depicts the amount of rabbit CAR mRNA expressed in LGAC treated with siRNA to CAR as well as a control (nonspecific) siRNA for 48 h. The CAR-specific siRNA sequences appeared to reduce the levels of CAR mRNA in LGAC relative to control siRNA. Separate controls (data not shown) revealed that CAR siRNA did not alter expression of a control gene (actin) and that control (nonspecific) siRNA did not affect CAR mRNA expression relative to that in untreated acini.

TABLE 1. Relative abundance of CAR mRNA in rabbit tissues[a]

Organ (control)	ΔC_T[b]	$\Delta\Delta C_T$[c]	Relative quantity
Liver 1 (HPRT1)	−2.50	0	1
	−1.77	0	1
LG 1 (HPRT1)	−2.15	−0.35	0.79
	−1.53	−0.24	0.85
Liver 2 (HPRT1)	−3.10	0	1
	−3.05	0	1
LG 2 (HPRT1)	−2.19	−0.91	0.53
	−2.36	−0.69	0.62
Liver 1 (PGK1)	4.18	0	1
	4.91	0	1
Spleen 1 (PGK1)	9.07	−4.89	0.034
	9.92	−5.02	0.031
Liver 2 (PGK1)	4.11	0	1
	4.15	0	1
Spleen 2 (PGK1)	10.96	−6.85	0.0087
	11.68	−7.54	0.0054

[a] Total RNAs were prepared from liver, lacrimal gland, and spleen from each of two rabbits, reverse transcribed, and then analyzed by real-time PCR using SYBR green as described in Materials and Methods. HPRT1 and PGK1 were selected as endogenous controls. Two pairs of CAR primers, listed in Materials and Methods, were used for the assay. Results for primer pair 1 appear in the top line for each sample (e.g., −2.50), and results for primer pair 2 appear in the bottom line for each sample (e.g., −1.77). Each reaction was conducted in triplicate, and the results were averaged.

[b] ΔC_T, difference in the threshold cycles of CAR mRNA and the control mRNA (HRPT1 or PGK1) within the same tissue.

[c] $\Delta\Delta C_T$, difference in the ΔC_T for liver and the ΔC_T for the experimental tissue, using the same primer.

FIG. 5. Rabbit CAR cDNA cloning. (A) CAR is expressed in rabbit LGAC as determined by RT-PCR. Total RNA was isolated from HeLa cells and mouse or rabbit LGAC, and cDNA was then synthesized as described in Materials and Methods. CAR gene expression was analyzed by PCR using primers designed according to a sequence conserved in human and mouse CAR. PCR products were separated on a 1.2% agarose gel. DNA bands of ~400 bp were sliced, extracted, and then further amplified by PCR, using the CAR primer shown above. A 437-bp rabbit CAR fragment, from which a 357-bp reliable sequence was acquired (not shown), was isolated from the gel and sequenced. (B) Total RNA was isolated from rabbit liver, rabbit LG, rabbit LGAC, or CHO cells, and CAR expression was determined by RT-PCR as for Fig. 5A. (C) The entire coding sequence of rabbit lacrimal acinar CAR was determined and compared with known CAR sequences from human and mouse. Total RNA was isolated from rabbit LGAC as described in Materials and Methods. The 5′ and 3′ fragments of rabbit CAR were produced by RACE PCR, using the specially designed 5′-end RACE primer, modified oligo(T) (3′), and CAR-specific downstream and upstream primers whose design was based on the 357-bp reliable sequence. 5′- and 3′-RACE fragments of CAR were extracted and subjected to DNA sequencing analysis. The resulting 1,695-bp rabbit CAR sequence includes the entire coding sequence of 1,098 bp, which was aligned with the known nucleotide sequences of human and mouse CAR, using an NCBI BLAST tool (bl2seq). Dashed boxes show the ATG start codon or TAG stop codon, and the closed box highlights the nucleotide sequences predicted to encode transmembrane helices in protein analyzed with the TMHMM method. Rabbit LGAC CAR has 89% sequence identity with human CAR and 83% sequence identity with mouse CAR. The rabbit LGAC CAR protein sequence was predicted by analyzing the 1,098-bp nucleotide sequence using the ORF finder from NCBI, resulting in the generation of a 365-amino-acid sequence, which was aligned with the known protein sequences of human and mouse CAR using an NCBI BLAST tool (blastp) (right). The closed box highlights the predicted transmembrane helices. Rabbit LGAC CAR has 89% amino acid sequence identity with human CAR and 88% amino acid sequence identity with mouse CAR.

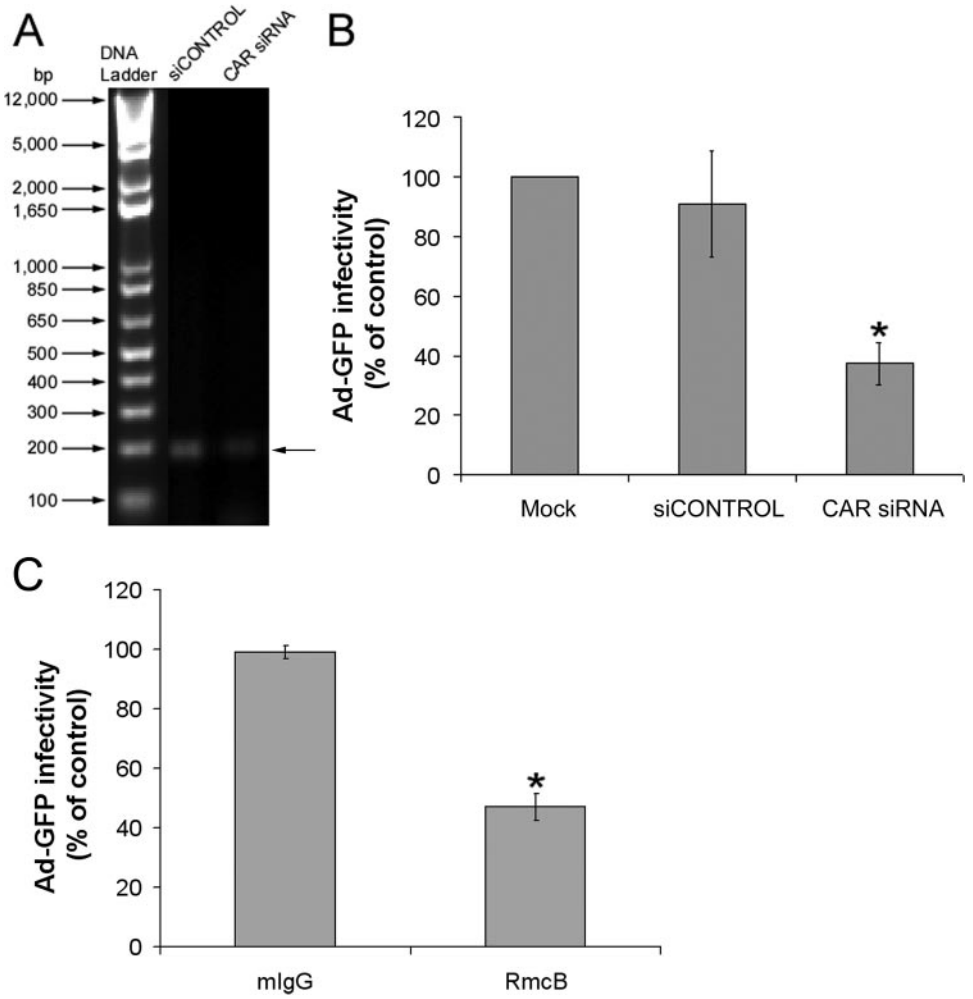

FIG. 6. Knockdown of CAR with CAR-specific siRNA but not nontargeting control siRNA. (A) Treatment of rabbit LGAC with CAR-specific siRNA resulted in significantly reduced expression of CAR. Rabbit LGAC seeded at a density of 2×10^6 cells/ml in 100-mm petri dishes were transfected with siRNA targeted to rabbit CAR or a siCONTROL nontargeting siRNA (100 nM) obtained from Dharmacon on day 1 of the culture, using the GeneSilencer siRNA transfection reagent. The CAR siRNA sense and antisense duplexes were designed according to the 1,098-bp CAR sequence shown in Fig. 5C with Dharmacon's online designer. After 48 h, the total RNA from the control and experimental cultures was isolated, treated, and used for cDNA synthesis as described in Materials and Methods. CAR gene expression in all samples was determined by PCRs within the linear range using primers designed according to the 1,098-bp rabbit lacrimal acinar CAR sequence. PCR products were separated on a 2% agarose gel. (B) Downregulation of CAR in rabbit LGAC reduced the transduction efficiency of Ad-GFP in those cells. Rabbit LGAC were seeded at a density of 1×10^6 cells/well and transfected with siRNA as described above. After 48 h, Ad-GFP was added at an MOI of 2 PFU/cell, and the cells were incubated for 1 h at 4°C before being rinsed and recovered and incubated for 10 to 12 h at 37°C. GFP positivity was determined by flow cytometry ($n = 4$). (C) Reduction in the amount of surface CAR available on HeLa cells reduced the transfection efficiency of Ad-GFP to a comparable level. HeLa cells seeded on uncoated 12-well plates at 1×10^5 cells/well and grown to 80% confluence were preincubated with anti-CAR RmcB monoclonal antibody or nonspecific mouse IgG (50 μg/ml) for 1 h at 4°C. Ad-GFP was added at an MOI of 2 PFU/cell, and the cells were incubated for 1 h at 4°C before being washed. The cells were then incubated for 10 to 12 h at 37°C. GFP positivity was determined by flow cytometry ($n = 4$). (*), significant at $P \leq 0.05$, based on results from mock-treated acini. Error bars represent the SEM.

To verify the effect of siRNA treatment, we quantified the change in CAR mRNA levels in CAR siRNA-treated LGAC relative to that for control (nonspecific) siRNA-treated LGAC using real time PCR as described in Materials and Methods. We detected a 30 to 35% reduction of CAR mRNA in the CAR siRNA-treated LGAC relative to that for untreated samples in two separate experiments using the PGK1 signal as an endogenous control. Under these conditions, equivalent control (nonspecific) siRNA elicited no marked changes in CAR mRNA levels (3 to 8% inhibition) relative to that for the untreated cells. Examination of the fluorescence signal associated with fluorescence-labeled oligonucleotides introduced under equivalent conditions showed that significant fluorescence could be detected in only 50% of LGAC ($n = 3$), suggesting that some cells took up less siRNA than others. Attempts to increase transfection efficiency by increasing the dose of added siRNA and/or transfection reagent were unsuccessful, resulting in increased cell toxicity even with control (nonspecific) siRNA.

Ad-GFP infection in LGAC (as a percentage of that in the control acini) exposed to control and CAR siRNA is shown in Fig. 6B. Control (nonspecific) siRNA did not affect Ad-GFP

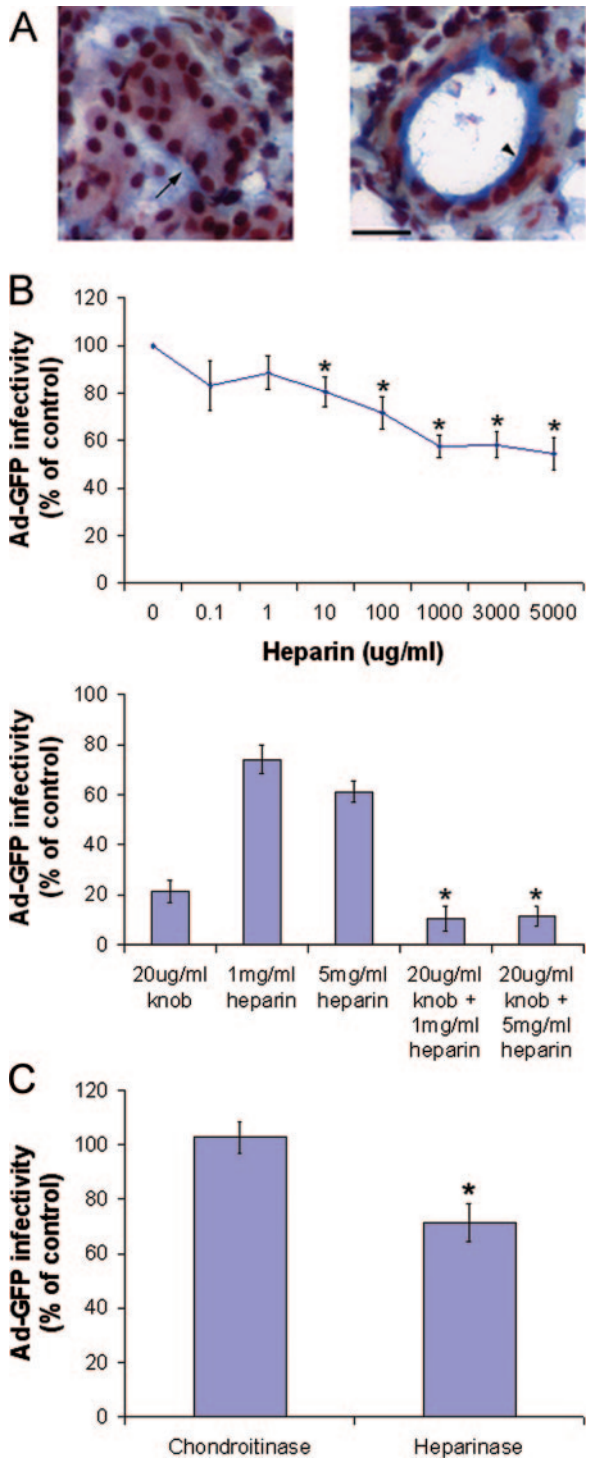

FIG. 7. Involvement of HS-GAGs in Ad5 transduction. (A) GAGs are abundant at the basolateral membranes of acinar cells and within ductal regions of the lacrimal gland. Rabbit lacrimal glands were removed and immersed in optimal cutting temperature medium, rapidly frozen with liquid nitrogen, and cryosectioned at 5 μm with a Mikrom cryostat. Cryosections on glass coverslips were processed for Russell-Movat's pentachrome staining. In both panels, the blue to green staining shows GAGs beneath the basolateral membrane of some acinar clusters (arrow in left panel) and in ductal regions (arrowhead in right panel). The black-stained areas are nuclei. Bar, 20 μm. (B) Treatment of Ad-GFP with heparin reduces infection efficiency by approximately 40%, and the effect is additive to that of knob rather than competitive. Rabbit LGAC were seeded onto Matrigel-coated 12-well plates at 2×10^6 cells/well. After 48 h, experimental cultures were incubated with recombinant knob protein (20 μg/ml) at an MOI of 2 PFU/cell and the controls were untreated. Ad-GFP that had been incubated with various concentrations of heparin for 1 h at 37°C was then added to control or experimental acinar cells for 1 h at 4°C. The cells were rinsed and incubated for 10 to 12 h at 37°C, and GFP positivity was determined by flow cytometry ($n = 4$). * in top panel, significant at $P \leq 0.05$ based on results for the control; * in bottom panel, significant at $P \leq 0.05$ based on results for knob-treated cells; error bars, SEM. (C) Treatment of rabbit LGAC with heparinases similarly reduced transduction efficiency of Ad-GFP. Rabbit LGAC were seeded onto Matrigel-coated 12-well plates at 2×10^6 cells/well and allowed to adhere for 3 h. A heparinase III cocktail (10 U/ml; a mixture of heparinases I, II, and III) or control chondroitinase ABC (10 U/ml) was incubated with the LGAC for 2 h at 37°C. The cells were then rinsed well, Ad-GFP was added, and the procedures described for panel B were followed ($n = 4$). *, significant at $P \leq 0.05$. Error bars represent the SEM.

infectivity relative to that for mock-treated acini, but treatment with the anti-CAR siRNA significantly reduced Ad-GFP infectivity, by about 60%. Morphological analysis revealed that LGAC exhibited no changes in cellular organization after siRNA treatment (data not shown). For comparison, inhibition of CAR function in HeLa cells by the RmcB anti-human CAR monoclonal antibody also significantly inhibited Ad5 transduction (Fig. 6C).

Evidence for HS-GAGs in Ad5 transduction into LGAC. Since fiber-dependent Ad5 transduction is extremely efficient, it seemed possible that Ad5 and fiber might utilize other receptors besides CAR to promote internalization in LGAC. Our previous studies and those of others have implicated HS-GAGs in the uptake of different viruses, including Ad2 and Ad5 in other cell types (14, 15, 20, 40). Since KKTK, a HS-GAG binding sequence, is contained in the Ad5 fiber shaft domain, we hypothesized that some Ad5 may enter LGAC by association with HS-GAGs. Figure 7A shows the result of MOVAT's pentachrome staining of the rabbit lacrimal gland, with the blue/green label indicating the abundant enrichment of GAGs. This labeling documented that GAGs were abundantly present at the basolateral membranes of acinar cells and within the ductal regions in lacrimal glands. To test the role of HS-GAGs in Ad5 entry, we preincubated Ad-GFP with heparin, an HS-GAG analog, to block the HS-GAG binding sites and then evaluated the effects on Ad-GFP transduction efficiency. As shown in Fig. 7B, heparin significantly inhibited Ad5-mediated gene transfer, up to a maximum of 40%, and inhibition was dose dependent. Heparin at doses of up to 5 mg/ml did not exert any changes on acinar cell viability or morphology (data not shown). Moreover, coadministration of heparin and knob elicited an additive inhibitory effect on Ad5 transduction, suggesting that in addition to CAR, HS-GAGs are involved in Ad5 attachment (Fig. 7B). As a control, chondroitin sulfate at doses of up to 5 mg/ml did not inhibit Ad5 transduction (data not shown), suggesting that this inhibitory effect was not due to simple charge interaction.

To further verify that the decrease in transduction efficiency was due to the blockade of Ad5 or fiber binding to PM HS-GAGs, not to nonspecific steric hindrance due to heparin binding to Ad5 or fiber, we also cleaved PM HS-GAGs, using a

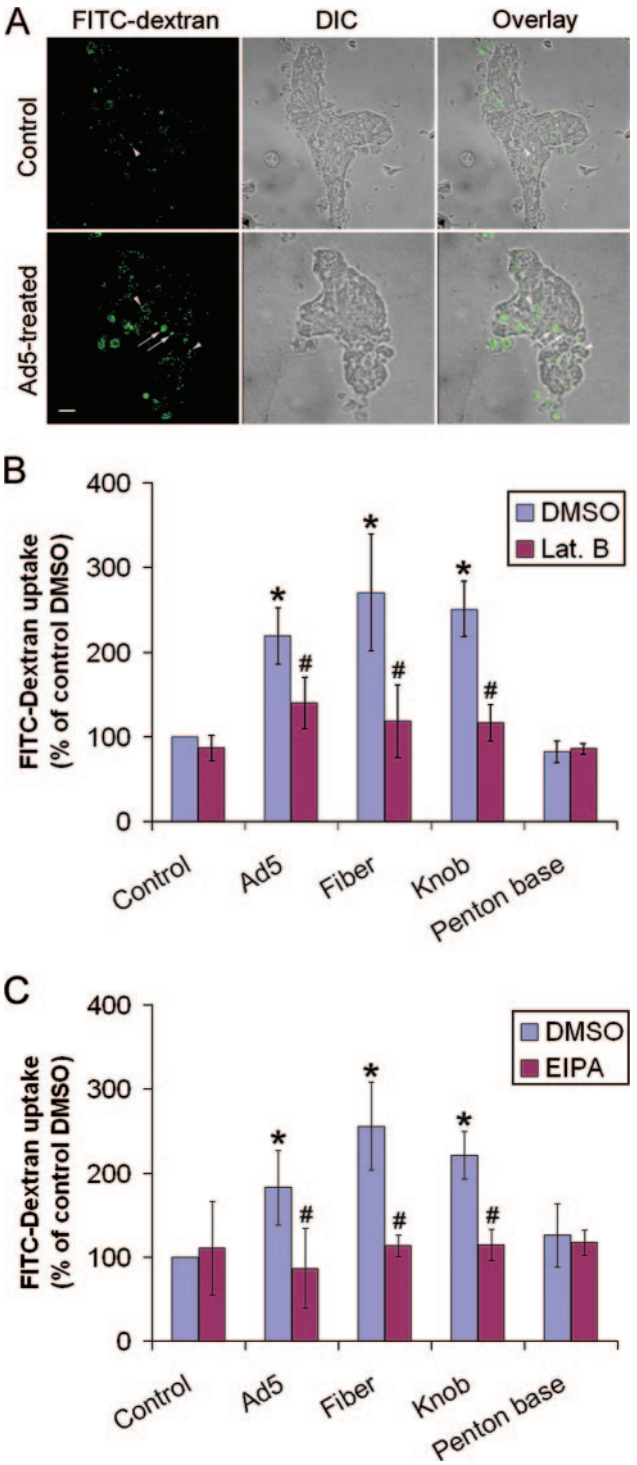

FIG. 8. Effects of Ad5 and capsid proteins on FITC-dextran uptake. (A) LGAC labeled with FITC-dextran, as a measure of macropinocytosis, were stimulated by exposure to Ad5. Rabbit LGAC were seeded onto Matrigel-coated 12-well plates at 2×10^6 cells/well. On day 3 of the culture, cells were incubated with or without Ad-LacZ (MOI = 100 PFU/cell) in binding buffer at 4°C for 1 h. The cells were washed, warmed to 37°C for 5 min, and pulsed with 1 mg/ml FITC-dextran at 37°C for 10 min. The cells were then washed extensively in ice-cold DPBS, fixed in 4% paraformaldehyde, and analyzed by confocal fluorescence microscopy. Arrowheads, accumulation of FITC-dextran in smaller intracellular vesicles (<1 μm); arrows, accumulation of FITC-dextran in larger intracellular vesicles (>1 μm); bar, 10 μm. (B) Significant reduction in Ad5-, fiber- or knob-stimulated FITC-dextran uptake with Lat B treatment suggests that Ad5-stimulated uptake is dependent on macropinocytosis. Rabbit LGAC were pretreated with DMSO or Lat B, incubated with Ad-LacZ or recombinant capsid proteins at cold temperatures, and analyzed for FITC-dextran uptake by flow cytometry as described in Materials and Methods. Penton base had no effect on uptake ($n = 4$). (C) Further confirmation that Ad5, fiber, and knob stimulate macropinocytosis was obtained by inhibiting virus-dependent uptake of FITC-dextran with the macropinocytosis inhibitor EIPA. Penton base had no effect on uptake. Rabbit LGAC were pretreated with DMSO or EIPA, incubated with Ad-LacZ or recombinant capsid proteins in cold temperatures, and analyzed for FITC-dextran uptake as described in Materials and Methods ($n = 5$). In panels B and C, * denotes significance at P values of ≤0.05 based on results for control acini and # denotes significance at P values of ≤0.05 based on results for the corresponding DMSO-treated acini.

cocktail of heparinases I, II, and III. These studies were conducted on freshly isolated lacrimal gland epithelial cells, since reconstitution into acinar clusters reduced the accessibility of the enzymes to HS-GAGs on the PM. As shown in Fig. 7C, these treatments also significantly inhibited Ad5 transduction efficiency (by ~30%). Treatment in parallel with chondroitinase ABC had no effect.

Ad5, fiber protein, and knob proteins stimulate macropinocytosis in LGAC. Macropinocytosis uses an endocytotic pathway in which ruffling PMs fuse to enclose surrounding fluids within 0.5- to 5.0-μm vacuoles that are then internalized by the cell (46). Macropinocytosis is thought to serve as a major mode of entry for viral transduction peptides like human immunodeficiency virus type 1 Tat protein (48) through their binding to HS-GAG-enriched PM (8, 47). It has been reported that Ad2 can elicit macropinocytosis in cultured cells (35). Therefore, it seemed possible that Ad5 fiber binding at the cell surface, particularly to HS-GAG- and/or CAR-enriched regions, might trigger macropinocytosis. The latter might then mediate at least an aspect of Ad5 internalization in acinar cells. To test this hypothesis, we investigated different hallmarks of macropinocytosis in LGAC with and without saturating amounts of Ad-LacZ. After 10 min, FITC-dextran showed substantial accumulation in large intracellular vesicles (≥1 μm), consistent with the size of the macropinosomes (Fig. 8). The intracellular accumulation of FITC-dextran in these structures appeared higher in LGAC treated with Ad-LacZ, suggesting that Ad5 may stimulate macropinocytosis in these cells.

Using flow cytometry, we measured FITC-dextran uptake in cells treated with and without Ad5, fiber, knob, or penton base protein. Ad5 significantly increased FITC-dextran uptake, an effect mimicked by fiber and knob but not the penton base. To determine if dextran uptake was sensitive to inhibition of macropinocytosis, we utilized both EIPA, an inhibitor of the Na/H exchanger and an established inhibitor of macropinocytosis (51), and Lat B, an inhibitor of actin filament reorganization which also inhibits macropinocytosis (3, 35). As expected, pretreatment of LGAC with either Lat B (10 μM) (Fig. 8B) or EIPA (500 μM) (Fig. 8C) completely blocked the FITC-dextran uptake stimulated by Ad5, fiber, and knob, suggesting that the increased FITC-dextran uptake was due to macropinocytosis. Consistent with this study, a previous report has used up

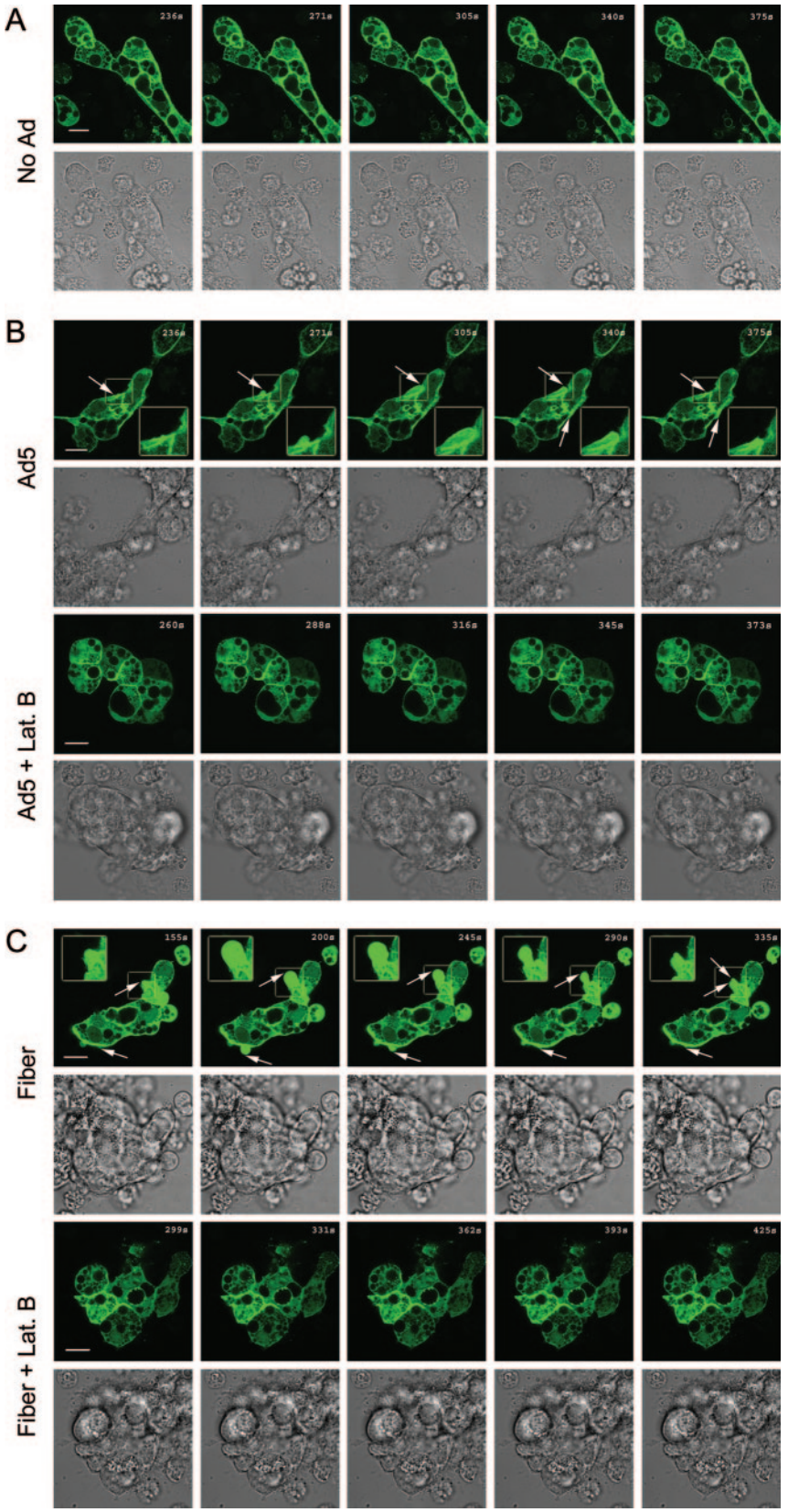

FIG. 9. Time-lapse confocal fluorescence microscopy of membrane ruffling in LGAC treated with Ad5 and capsid proteins. Rabbit LGAC transduced to express GFP-actin as described in Materials and Methods were treated with DMSO or Lat B prior to being incubated with Ad-LacZ (MOI = 100 PFU/cell) or recombinant fiber (20 μg/ml) at 4°C for 1 h. The cells were warmed at 37°C for 5 min prior to the onset of the time-lapse sequence. Selected GFP-actin fluorescence and DIC images at regular intervals throughout the time-lapse sequence are shown. The arrows indicate basolateral actin remodeling. The boxed images were magnified and are shown in the insets. Bars, 10 μm.

to 1 mM EIPA to fully inhibit Na^+/H^+ activity in LGAC (38). Neither of these agents elicited significant toxicity at the concentrations used: trypan blue exclusion verified that EIPA-treated LGAC (500 μM; 2 h) exhibited viability that was 88% ± 1% of that of untreated LGAC while Lat B-treated LGAC (10 μM; 2 h) exhibited viability that was 95% ± 1% of that of untreated LGAC ($n = 4$).

Ad5, fiber, and knob elicit actin filament ruffling. Rearrangement of the actin cytoskeleton is another characteristic of macropinocytosis (35, 46). Macropinosomes are formed from cell surface membrane ruffles folding back on the PM, a process critically dependent on actin filaments. To further test whether Ad5, fiber, and knob elicited the actin rearrangement characteristic of macropinocytosis, we analyzed GFP-actin dynamics by time-lapse confocal fluorescence microscopy in acinar cells treated with Ad5, fiber, knob, or penton base protein or not treated. As shown in Fig. 9, GFP-actin coassembles with endogenous actin into filaments enriched beneath apical and basolateral PMs. Compared to control cells which showed little change in actin organization at the PM (Fig. 9A), Ad5-treated cells showed extensive basolateral membrane ruffling (Fig. 9B, rows 1 to 2). Similar membrane-ruffling processes were observed in cells treated with fiber (Fig. 9C, rows 1 to 2) and knob (images not shown). In contrast, penton base-treated cells did not exhibit basolateral PM ruffling nor any other actin-associated change (images not shown). Control proteins purified within the same background as the fiber (GST produced by baculovirus infection of Sf9 cells) and the knob (rab3DQL produced in *E. coli*) did not elicit any membrane ruffling (images not shown). Lat B pretreatment completely blocked the basolateral PM ruffling induced by Ad5 (Fig. 9B, rows 3 and 4), fiber (Fig. 9C, rows 3 and 4), or knob (data not shown), verifying that the observed dynamic membrane ruffling was due specifically to actin filament remodeling.

Since a previous report has linked macropinocytosis and membrane ruffling to exposure to the penton base protein (35), we wanted to quantify the extent of actin filament ruffling elicited by Ad5 and each of its capsid proteins to validate the impression that these activities were associated with the fiber protein and not the penton base protein. We did this by measuring the maximum diameter of all membrane extensions observed during a 10-min interval over multiple preparations under each condition. A representative field with several membrane extensions in various stages of formation or retraction is shown in Fig. 10A, while Fig. 10B represents the average number of events of specific diameter per field under different experimental conditions. In untreated acini, a low level of membrane extension/ruffling was typically observed, and almost all of these extensions were small in diameter. The number of membrane-ruffling events and the maximum diameter of the membrane-ruffling events were significantly increased by Ad5, fiber, and knob treatment but not by penton base treatment. Figure 10C shows that control proteins purified in the same background as fiber protein (GST) and knob (Rab3DQL) did not increase membrane ruffling.

Macropinocytosis contributes to Ad5 infection efficiency but is not directly involved in viral entry. To address the role of macropinocytosis in the fiber-dependent internalization of Ad5 in LGAC, we investigated the effects of EIPA and Lat B on Ad5 transduction efficiency. As shown in Fig. 11A, pretreatment of LGAC with EIPA or Lat B significantly inhibited Ad-GFP infectivity, suggesting that an aspect of Ad5 transduction into LGAC involved macropinocytosis. Analysis in parallel of Ad5 internalization under these conditions using the acquisition of trypsin resistance by fiber protein as a marker of virus internalization revealed that the amount of Ad5 fiber protein internalized at 60 min with or without EIPA or Lat B treatment was comparable (Fig. 11B). These data suggested that the process of fiber-induced macropinocytosis was important for efficient Ad5 transduction of LGAC but that the Ad5 itself did not enter the cells via macropinosomes.

To further resolve the mechanism of internalization of Ad5 in LGAC, we examined the extent of internalized Ad5 colocalized with markers of different endocytotic pathways. Figure 12A shows that Ad5 internalized in the presence of FITC-dextran exhibits essentially no colocalization with macropinosomes after 10 min of exposure. A similar lack of colocalization was seen for time periods between 5 and 60 min. In addition, Ad5 internalized in parallel with fluorescent cholera toxin subunit B also showed no colocalization, further suggesting that Ad5 did not enter LGAC through caveolae (data not shown). Internalized Ad5 showed significant colocalization with the early endosomal marker EEA1, which receives traffic from the clathrin-mediated endocytotic pathway. Colocalization was seen as early as 5 to 10 min after Ad5 uptake was begun and increased for up to 60 min (Fig. 12B). This finding suggests that Ad5 entry into LGAC, although fiber-dependent, occurs via the clathrin-dependent endocytotic pathway.

DISCUSSION

In this study we have explored the uptake mechanism utilized for LGAC internalization of Ad5. Our results suggest that Ad5 internalization in LGAC is largely fiber dependent and that the knob may be able to mimic aspects of the Ad5 internalization pathway. Both CAR and HS-GAGs are implicated in fiber-dependent transduction of LGAC by Ad5. Although macropinocytosis is also elicited by fiber and appears to play a functional role in Ad5 transduction of LGAC, our data suggest that macropinocytosis is unlikely to serve as the route of entry for Ad5 into these cells. Rather, internalized Ad5 is most extensively colocalized with early endosomes enriched in EEA1, which receive clathrin-mediated endocytotic traffic. The macropinocytosis data collectively suggest that this process is not directly responsible for Ad5 or fiber uptake; instead, macropinocytosis or a downstream event may regulate intracellular trafficking of Ad5 once it is internalized.

In most cells investigated, endocytosis of Ad5 is mediated by the penton base protein, while the fiber is responsible only for initial cell attachment. In fact, in many cells the recombinant penton base proteins from Ad2 (28) or Ad5 (41) are by themselves capable of cell attachment, endocytosis, endosomolysis, enhanced nuclear targeting, and nuclear entry. Surprisingly, recombinant penton base associates with the PM of LGAC, as shown by confocal fluorescence microscopy and biochemical assays, but does not appear to be internalized. Our previous work has established that the penton base protein remains surface associated in LGAC for up to 24 h (24), suggesting a sustained interaction with a receptor(s) that may not turn over on the PM very rapidly. The data reported herein on lack of

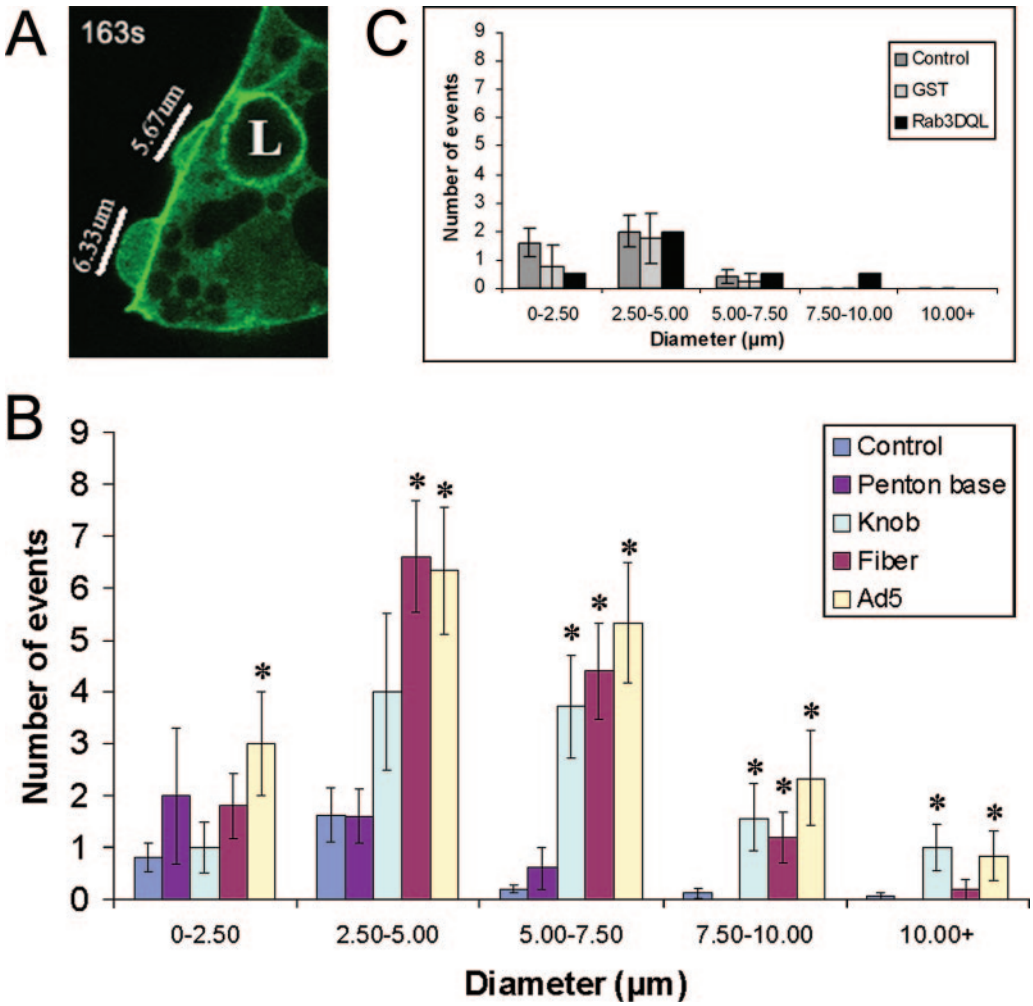

FIG. 10. Quantitation of membrane-ruffling events elicited by Ad5 and capsid proteins in LGAC. (A) A representative image of a transduced LGAC exposed to Ad-LacZ (MOI = 100 PFU/cell) from one frame within the 600-s analysis period is shown. The diameters of several membrane extensions in different stages of development are marked. (B) Treatment of LGAC with Ad5, fiber, and knob cause a significant increase in the number and size of membrane-ruffling events, while treatment with penton base does not. The histogram plot shows an average of the number of membrane-ruffling events per sequence (600-s analysis of an acinar cluster) under each experimental condition, with the ruffling events further grouped by maximum diameter. Data were collected from acinar clusters of comparable cell number and transduction efficiency within a 600-s period representing the period of highest membrane-ruffling activity in each sequence. Each membrane protrusion event occurring within that time frame was recorded at its largest diameter, using the LSM Image Browser overlay tools to measure diameter. These values were then classified by treatment group and divided into different maximal diameter ranges. The number of ruffling events in each range was grouped by treatment and divided by the number of sequences analyzed to obtain an average value per sequence for each treatment. Rabbit LGAC transduced to express GFP-actin as described in Materials and Methods were treated with recombinant proteins (20 μg/ml) or Ad-LacZ (MOI = 100 PFU/cell) at 4°C for 1 h and warmed at 37°C for 5 min prior to the onset of image acquisition ($n = 16$ for the control; $n = 5$ for penton base; $n = 7$ for knob; $n = 5$ for fiber; and $n = 6$ for Ad5). Panel C shows comparable values obtained from controls ($n = 5$), GST ($n = 4$), and Rab3DQL ($n = 2$). *, significant at $P \leq 0.05$ based on results for the control. Error bars represent the SEM.

penton internalization, combined with our previous findings on the longevity of the penton association with the acinar PM, suggest that the penton base protein of Ad5 may play a role in primary attachment to a surface receptor in LGAC, analogous to the role of the fiber-CAR interaction in other cells.

One question of obvious interest is the identity of the penton base binding partner or partners in LGAC. Unlike hepatocytes, LGAC do express α_v integrins. However, the trafficking dynamics of integrins in LGAC, which are differentiated secretory epithelial cells, may be quite different than in the adherent HeLa cell monolayers known to internalize Ad5 through integrin-mediated endocytosis. In LGAC, α_v integrins may be less abundant or relatively inaccessible to added penton base or Ad5, allowing its association with other proteins. Within this context, confocal fluorescence microscopy revealed that after 60 min recombinant penton base protein with a mutation introduced into the RGD binding site responsible for α_v integrin binding (41) showed a level of association with LGAC PM comparable to that for the wild-type penton base protein (data not shown).

The question then arises as to what alternative receptor or receptors may the fiber protein associate with that can mediate Ad5 internalization in LGAC. Only one other cell type has previously been reported to utilize a penton base-independent

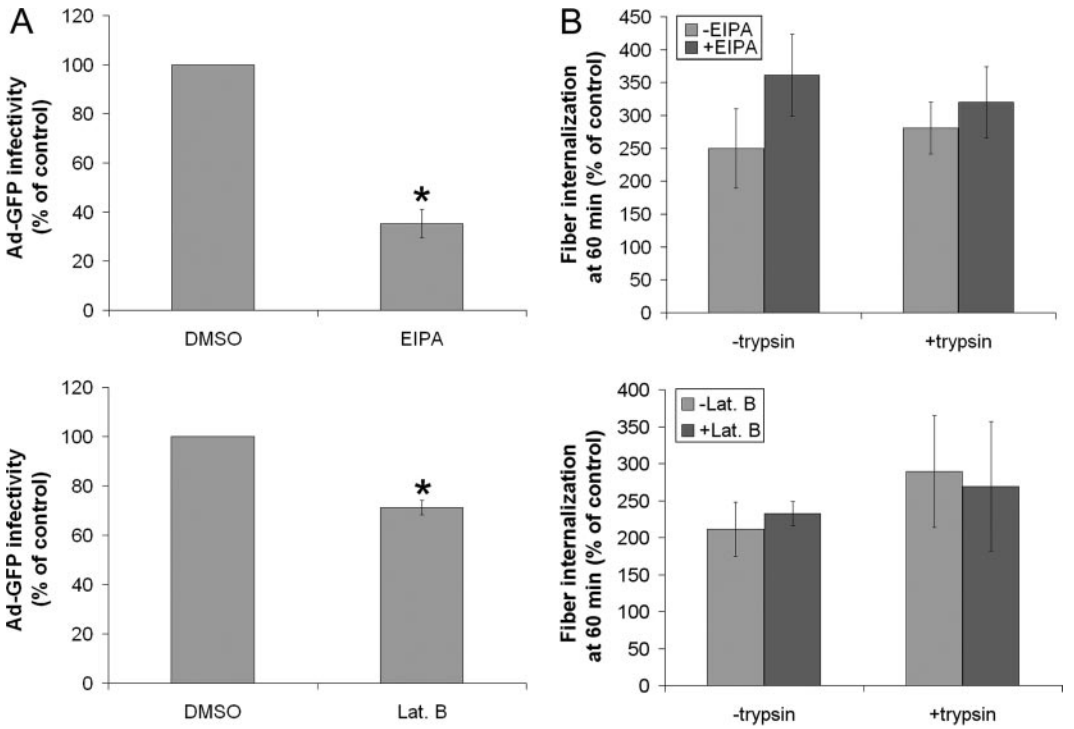

FIG. 11. Effect of EIPA and Lat B on Ad5 infection efficiency and fiber entry. (A) Treatment with EIPA and Lat B significantly reduces Ad5 infection efficiency, suggesting that macropinocytosis may play a role in the infection process. Rabbit LGAC were seeded onto Matrigel-coated 12-well plates at 2×10^6 cells/well. On day 2 of the culture, acinar cells were preincubated with DMSO, 500 μM EIPA, or 10 μM Lat B for 1 h at 37°C. Ad-GFP was then added at an MOI of 2 PFU/cell, and the cells were incubated for 1 h at 4°C before being washed and incubated for 10 to 12 h at 37°C. GFP positivity was determined by flow cytometry ($n = 4$ for EIPA; $n = 5$ for Lat B). *, significant at $P \leq 0.05$ based on results for DMSO-treated acini. Error bars represent the SEM. (B) Inhibitors of macropinocytosis do not prevent fiber entry. Rabbit LGAC were seeded in 150-mm petri dishes at a density of 2×10^6 cells/ml. On day 2 of the culture, vehicle-treated rabbit LGAC or LGAC pretreated with either Lat B or EIPA as described for panel A were incubated with Ad5 at an MOI of 15 PFU/cell for 0 or 60 min, followed by treatment with 0.2 mg/ml trypsin-EDTA for 1 h at 4°C and lysis using RIPA buffer. Cell lysates (150 μg/lane) were blotted with monoclonal antibody to fiber protein and IRDye800-conjugated secondary antibody ($n = 3$). Error bars represent the SEM. Values shown are fiber protein uptake at 60 min relative to that for the control (0 min, incubated only with Ad5).

internalization mechanism for Ad5: hepatocytes, which lack expression of $\alpha_v\beta_3$ and $\alpha_v\beta_5$ integrins (26). When radioiodinated fiber knob is administered intravenously to mice, it is cleared into an intracellular degradative compartment in the liver, suggesting that knob is internalized through binding to a cellular receptor, followed by endocytosis (2). Since knob exhibits strong CAR binding and CAR is highly abundant in liver, one possibility suggested by these investigators is that CAR mediates internalization of knob in hepatocytes, although this has not been directly tested. Awasthi et al. (2) have further speculated that the abundant CAR expression in liver may allow association of this protein with diverse membrane domains, including not only adhesion sites but also domains associated with endocytotic uptake. Like hepatocytes, which also utilize an integrin-independent Ad5 infection pathway, LGAC are efficiently transduced by Ad5, take up knob protein into intracellular compartments, and exhibit a very high level of CAR expression.

In many cells, CAR has been widely studied as a viral receptor important in Ad5 surface attachment prior to internalization. Consistent with this, when we pretreated HeLa cells with the RmcB antibody to human CAR, we significantly reduced the ability of these cells to be transduced by Ad5. In LGAC, a reduction in CAR mRNA elicited through siRNA treatment also caused a significant reduction in Ad5 transduction. This effect could be due to reduced Ad5 attachment to CAR, consistent with the model of inhibition elicited in HeLa cells by the RmcB antibody. Alternatively, the inhibitory effect could be due to a reduction of a specific population of recycling CAR in LGAC that is actually responsible for Ad5 endocytosis. Such a population might exist in cells expressing a significant amount of CAR, such as liver and lacrimal gland, as mentioned above (2).

It is also intriguing that the inhibitory effect of CAR knockdown by siRNA on Ad-GFP transduction was greater (60%) than the actual reduction in CAR mRNA levels verified by real-time PCR (30 to 35%). Conceivably, if there are multiple functional pools of CAR in tissues that express significant amounts of this protein, a reduction in CAR mRNA may selectively deplete one functional pool. For instance, if CAR is implicated in LGAC in both cell adhesion and endocytotic recycling, a reduction in CAR mRNA levels might selectively deplete the endocytotic recycling pool if the junctional CAR pool is preferentially targeted. In addition, if each molecule of CAR is responsible for internalization of multiple Ad5 virions through uptake, release, and endocytotic recycling, a lack of

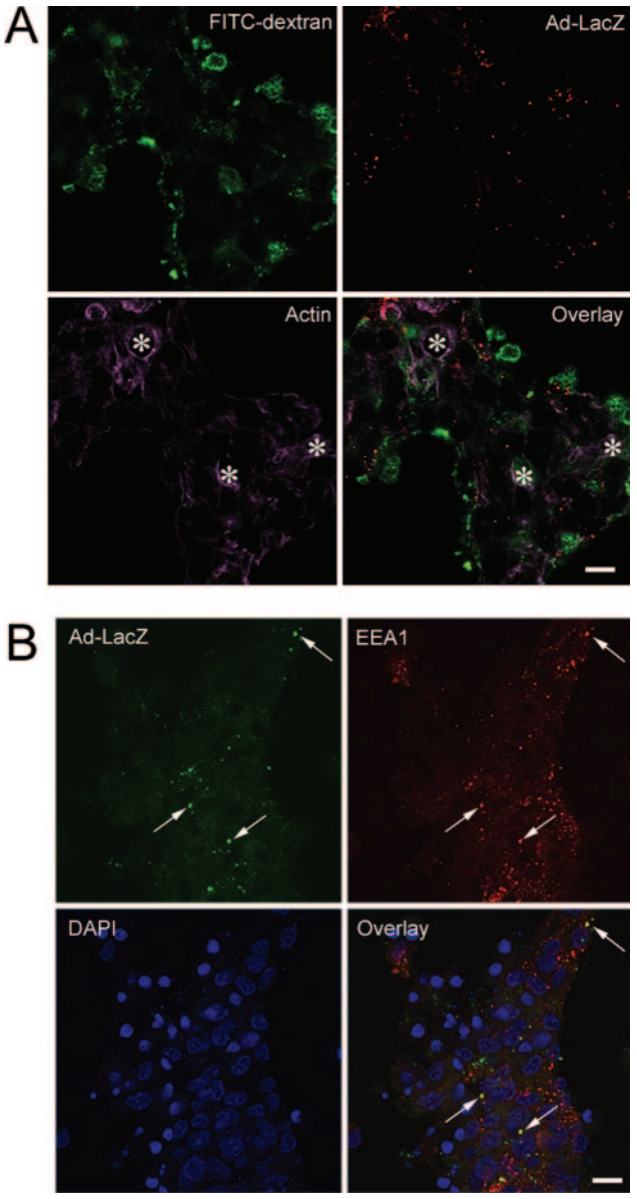

FIG. 12. Colocalization of endocytotic markers with Ad5. (A) Localization of Ad5 after internalization reveals that its intracellular trafficking pathway diverges from the macropinocytosis pathway. Rabbit LGAC were seeded onto Matrigel-coated 12-well plates at 2×10^6 cells/well. On day 3 of the culture, the cells were incubated with or without Ad-LacZ (MOI = 100 PFU/cell) in binding buffer at 4°C for 1 h. The cells were washed, warmed to 37°C for 5 min, and pulsed with 1 mg/ml FITC-dextran at 37°C for 10 min. The cells were then washed extensively in ice-cold DPBS, fixed in 4% paraformaldehyde, and processed to fluorescence label FITC-dextran (green), Ad5 proteins (red), and actin filaments (purple). A similar lack of colocalization was seen when lower doses of Ad5 were applied. *, apical/luminal region; bar, 10 μm. (B) Fiber-dependent Ad5 entry into LGAC appears to occur via the clathrin-dependent endocytotic pathway. Rabbit LGAC were seeded onto Matrigel-coated 12-well plates at 2×10^6 cells/well. On day 3 of the culture, the cells were exposed to Ad-LacZ (MOI = 40 PFU/ml) for 60 min before being fixed and processed to fluorescence label Ad5 proteins (green), EEA1 (red), and nuclei (blue). The arrows point to a few of the many areas of colocalization of Ad5 and EEA1. Bar, 10 μm. A similar colocalization was seen when higher doses of Ad5 were applied (MOI up to 100 PFU/cell).

1:1 correspondence in receptor number and transduction efficiency would be expected.

In addition to the abundant expression of CAR in two tissues which utilize a penton-independent uptake mechanism for Ad5, a few other observations reinforce the possibility of a distinct pool of recycling CAR that may mediate Ad5 uptake in certain cells. First, one study has reported that the carboxy terminal tail domain of CAR appears to confer its localization to a novel lipid raft domain that also contains the low-density-lipoprotein receptor and that these two receptors share the YXXϕ motif associated with adapter protein binding during clathrin-mediated endocytosis (1). Moreover, recent work examining the internalization of a CAR-dependent strain of coxsackie B virus in HeLa cells has shown that coxsackie B virus binding stimulates internalization of CAR and its colocalization with clathrin and EEA1, suggesting that CAR mediates the endocytotic uptake of the coxsackie B virus under some conditions (7). Finally, although there is strong homology between human and rabbit acinar CAR, none of the commercial anti-human CAR antibodies, including the function-blocking anti-human CAR RmcB antibody, showed sufficient immunoreactivity by Western blotting or surface binding by flow cytometry to any 46-kDa species in lacrimal gland representing the major CAR isoform in other systems. Western blotting with the rabbit polyclonal anti-human CAR antibody recognized a lower-molecular mass species (18 kDa) in rabbit acinar lysates that was also present in HeLa lysates (data not shown), suggesting that an alternative splice form of CAR may be present in LGAC. A CAR splice variant might exhibit different properties that would enable it to mediate Ad5 endocytosis in LGAC. The possibility that CAR directly mediates Ad5 endocytosis through interaction with fiber is intriguing. We cannot exclude the possibility that CAR simply facilitates Ad5 attachment to the PM of LGAC through fiber binding, comparable to other cell models, while another as yet unknown protein mediates fiber-based Ad5 internalization.

We also found that inhibition of HS-GAG binding either through use of heparin or by the enzymatic removal of surface HS-GAGs partially blocks Ad5 transduction. The inhibitory effect of heparin is incomplete (~30 to 40%) but is additive with knob. Finding an additive inhibitory effect of fiber and heparin suggests that the primary fiber receptor is not an HS-GAG, but rather that HS-GAG binding may enhance virus attachment as a secondary receptor, thus facilitating virus entry. The Ad5 fiber shaft domain contains the conserved basic peptide sequence KKTK, a motif that has been proposed to be responsible for the binding of fiber to HS-GAGs and acidic carbohydrates (14, 15, 20). This additive effect of heparin and knob is also consistent with the possible interaction of the KKTK site in the fiber shaft with HS-GAGs, while the knob domain interacts with another receptor, possibly CAR. In most but not all cases, HS-GAGs play a major role in adhesion of virus to the PM rather than in the internalization process. It is possible that the immobilization of the virus during the initial adhesion to surface HS-GAGs allows the virus better access to other cellular receptors that are required for internalization. It has also been postulated that binding to HS-GAG may be the factor that allows the accumulation of appropriate receptors adjacent to the HS binding site (45).

Consistent with previous work by Meier et al. with HeLa

cells (35), our results indicate that Ad5 can stimulate actin filament remodeling associated with enhanced macropinocytosis in LGAC. Activation of macropinocytosis in HeLa cells occurs when Ad2 binding signals activation of phosphatidylinositol 3-kinase, protein kinase C, and the rho GTPase Rac1 (35). Presumably this signaling cascade is stimulated by the Ad2 penton base protein binding to α_v integrins in these cells, although this was not directly tested with purified or recombinant penton base protein. Our data strongly suggest that stimulation of macropinocytosis in LGAC is mediated by fiber, since the effect of Ad5 can be mimicked by either recombinant fiber or knob protein but not penton base. It is unclear at the present time whether fiber binding in LGAC can stimulate some of the same downstream signaling pathways that were implicated in Ad2-induced macropinocytosis in HeLa cells or whether the process in LGAC occurs via a unique mechanism.

Recent evidence has implicated HS-GAG binding in activation of macropinocytosis in some systems (8, 47, 48). In fact, the cytoplasmic domains of HS-GAG-associated proteins have been shown to interact with the actin cytoskeleton (56). If this interaction is responsible for the induction of macropinocytosis, it is somewhat surprising that knob can stimulate macropinocytosis, since knob lacks the KKTK motif present on the fiber shaft domain that is proposed to interact with HS-GAG-enriched regions. There may in fact be additional sequences that serve as HS-GAG binding motifs that are thus far unidentified.

In summary, this study provides evidence that Ad5 exploits a novel series of interactions among several different binding partners to facilitate viral entry into LGAC, in comparison with the penton-based mechanisms described for many other cells, including HeLa cells. CAR and HS-GAGs appear to participate in fiber-driven Ad5 entry into LGAC, although their precise role (e.g., binding and/or internalization) remains unknown. Likewise, fiber-induced macropinocytosis appears to be functionally important in Ad5 transduction, likely by enhancing intracellular trafficking rather than by internalization of Ad5. Surprisingly, the penton base protein which appears to determine the Ad5 internalization route in many other cell types remains associated with the PM and is unable to recapitulate the Ad5 entry pathway in LGAC. Our work illustrates the importance of investigating the mechanisms of viral entry and intracellular trafficking in diverse cell types, including those such as LGAC which may more closely resemble the physiological targets for viral and nonviral gene therapy than commonly studied cell lines like HeLa cells.

ACKNOWLEDGMENTS

This work was supported by NIH grants EY-13949 and EY-17293 to S.F.H.-A. and by grant P30 DK-48522 (Confocal Microscopy and Molecular Biology Subcores, USC Center for Liver Diseases). Additional salary support to S.F.H.-A. was from NIH grants EY-11386, EY-05081, NS-38246, and DK-34316.

We thank Wei-Chiang Shen and Raj Batra for helpful discussions.

REFERENCES

1. **Ashbourne Excoffon, K. J. D., T. Moninger, and J. Zabner.** 2003. The coxsackie B virus and adenovirus receptor resides in a distinct membrane microdomain. J. Virol. **77:**2559–2567.
2. **Awasthi, V., G. Meinken, K. Springer, S. C. Srivastava, and P. Freimuth.** 2004. Biodistribution of radioiodinated adenovirus fiber protein knob domain after intravenous injection in mice. J. Virol. **78:**6431–6438.
3. **Baluska, F., J. Samaj, A. Hlavacka, J. Kendrick-Jones, and D. Volkmann.** 2004. Actin-dependent fluid-phase endocytosis in inner cortex cells of maize root apices. J. Exp. Bot. **55:**463–473.
4. **Bergelson, J. M., J. A. Cunningham, G. Droguett, E. A. Kurt-Jones, A. Krithivas, J. S. Hong, M. S. Horwitz, R. L. Crowell, and R. W. Finbert.** 1997. Isolation of a common receptor for coxsackie B viruses and adenoviruses 2 and 5. Science **275:**1320–1323.
5. **Borras, T.** 2003. Recent developments in ocular gene therapy. Exp. Eye Res. **76:**643–652.
6. **Caplen, N. J., S. Parrish, F. Imani, A. Fire, and R. A. Morgan.** 2001. Specific inhibition of gene expression by small double-stranded RNAs in invertebrate and vertebrate systems. Proc. Natl. Acad. Sci. USA **98:**9742–9747.
7. **Chung, S. K., J. Y. Kim, I. B. Kim, S. I. Park, K. H. Paek, and J. H. Nam.** 2005. Internalization and trafficking mechanisms of coxsackievirus B3 in HeLa cells. Virology **333:**31–40.
8. **Console, S., C. Marty, C. Garcia-Echeverria, R. Schwendener, and K. Ballmer-Hofer.** 2003. Antennapedia and HIV transactivator of transcription (TAT) "protein transduction domains" promote endocytosis of high molecular weight cargo upon binding to cell surface glycosaminoglycans. J. Biol. Chem. **278:**35109–35114.
9. **Cordeiro, M. F., G. S. Schultz, R. R. Ali, S. S. Bhattacharya, and P. T. Khaw.** 1998. Molecular therapy in ocular wound healing. Br. J. Ophthalmol. **83:**1219–1224.
10. **Coyne, C. B., and J. M. Bergelson.** 2005. CAR: a virus receptor within the tight junction. Adv. Drug Deliv. Rev. **57:**869–882.
11. **da Costa, S. R., E. Sou, J. Xie, F. A. Yarber, C. T. Okamoto, M. Pidgeon, M. M. Kessels, A. K. Mircheff, J. E. Schechter, B. Qualmann, and S. F. Hamm-Alvarez.** 2003. Impairing actin filament or syndapin functions promotes accumulation of clathrin-coated vesicles at the apical plasma membrane of acinar epithelial cells. Mol. Biol. Cell **14:**4397–4413.
12. **da Costa, S. R., F. A. Yarber, L. Zhang, M. Sonee, and S. F. Hamm-Alvarez.** 1998. Microtubules facilitate the stimulated secretion of beta-hexosaminidase in lacrimal acinar cells. J. Cell Sci. **111:**1267–1276.
13. **Dartt, D. A.** 1994. Signal transduction and activation of the lacrimal gland, p. 458–465. *In* D. M. Albert and F. A. Jacobiec (ed.), Principles and practice of ophthalmology, 2nd ed. Saunders, Philadelphia, Pa.
14. **Dechecchi, M. C., P. Melotti, A. Bonizzato, M. Santacatterina, M. Chilosi, and G. Cabrini.** 2001. Heparan sulfate glycosaminoglycans are receptors sufficient to mediate the initial binding of adenovirus types 2 and 5. J. Virol. **75:**8772–8780.
15. **Dechecchi, M. C., A. Tamanini, A. Bonizzato, and G. Cabrini.** 2000. Heparan sulfate glycosaminoglycans are involved in adenovirus type 5 and 2-host cell interactions. Virology **268:**382–390.
16. **Elbashir, S. M., J. Harborth, W. Lendeckel, A. Yalcin, K. Weber, and T. Tuschl.** 2001. Duplexes of 21-nucleotide RNAs mediate RNA interference in cultured mammalian cells. Nature **411:**494–498.
17. **Fechner, H., A. Haack, H. Wang, X. Wang, K. Eizema, M. Pauschinger, R. G. Schoemaker, R. van Veghel, A. B. Houtsmuller, H. P. Schultheiss, M. J. Lamers, and W. Poller.** 1999. Expression of Coxsackie adenovirus receptor and alpha$_v$-integrin does not correlate with adenovector targeting in vivo indicating anatomical vector barriers. Gene Ther. **6:**1520–1535.
18. **Fox, R. I., M. Stern, and P. Michelson.** 2000. Update in Sjögren's syndrome. Curr. Opin. Rheumatol. **12:**391–398.
19. **Fullard, R.** 1994. Tear proteins arising from lacrimal tissue, p. 473–479. *In* D. M. Albert and F. A. Jacobiec (ed.), Principles and practice of ophthalmology, 2nd ed. Saunders, Philadelphia, Pa.
20. **Gaden, F., L. Franqueville, S. S. Hong, V. Legrand, C. Figarella, and P. Boulanger.** 2002. Mechanisms of restriction of normal and cystic fibrosis transmembrane conductance regulator-deficient human tracheal gland cells to adenovirus infection and Ad-mediated gene transfer. Am. J. Respir. Cell Mol. Biol. **27:**628–640.
21. **Gierow, J. P., S. Andersson, and E. C. Sjogren.** 2002. Presence of alpha- and beta-integrin subunits in rabbit lacrimal gland acinar cells cultured on a laminin-rich matrix. Adv. Exp. Med. Biol. **506:**59–63.
22. **Gierow, J. P., R. W. Lambert, and A. K. Mircheff.** 1995. Fluid phase endocytosis by isolated rabbit lacrimal gland acinar cells. Exp. Eye Res. **60:**511–525.
23. **Greber, U. F., M. Willetta, P. Webster, and A. Helenius.** 1993. Stepwise dismantling of adenovirus 2 during entry into cells. Cell **75:**477–486.
24. **Hamm-Alvarez, S. F., S. da Costa, T. Yang, X. Wei, J. P. Gierow, and A. K. Mircheff.** 1997. Cholinergic stimulation of lacrimal acinar cells promotes redistribution of membrane-associated kinesin and the secretory protein, β-hexosaminidase, and increases kinesin motor activity. Exp. Eye Res. **64:**141–156.
25. **Hamm-Alvarez, S. F., J. Xie, Y. Wang, and L. K. Medina-Kauwe.** 2003. Modulation of secretory functions in epithelia by adenovirus capsid proteins. J. Control. Release **93:**129–140.
26. **Hautala, T., T. Grunst, A. Fabrega, P. Freimuth, and M. J. Welsh.** 1998. An interaction between penton base and αv integrins plays a minimal role in adenovirus-mediated gene transfer to hepatocytes in vitro and in vivo. Gene Ther. **5:**1259–1264.
27. **Henry, L. J., D. Xia, M. E. Wilke, J. Deisenhofer, and R. D. Gerard.** 1994.

Characterization of the knob domain of the adenovirus type 5 fiber protein expressed in *Escherichia coli*. J. Virol. **68:**5239–5246.
28. **Hong, S. S., B. Gay, L. Karayan, M.-C. Dabauvalle, and P. Boulanger.** 1999. Cellular uptake and nuclear delivery of recombinant adenovirus penton base. Virology **262:**163–177.
29. **Jerdeva, G. V., K. Wu, F. A. Yarber, C. J. Rhodes, D. Kalman, J. E. Schechter, and S. F. Hamm-Alvarez.** 2005. Actin and non-muscle myosin II facilitate apical exocytosis of tear proteins in rabbit lacrimal acinar epithelial cells. J. Cell Sci. **118:**4797–4812.
30. **Jerdeva, G. V., F. A. Yarber, M. D. Trousdale, C. J. Rhodes, C. T. Okamoto, D. A. Dartt, and S. F. Hamm-Alvarez.** 2005. Dominant-negative PKC-epsilon impairs apical actin remodeling in parallel with inhibition of carbachol-stimulated secretion in rabbit lacrimal acini. Am. J. Physiol. Cell Physiol. **289:**C1052–C1068.
31. **Medina-Kauwe, L. K.** 2003. Endocytosis of adenovirus and adenovirus capsid proteins. Adv. Drug Deliv. Rev. **55:**1485–1496.
32. **Medina-Kauwe, L. K., and X. Chen.** 2002. Using GFP–ligand fusions to measure receptor-mediated endocytosis in living cells. Vitam. Horm. **65:**81–95.
33. **Medina-Kauwe, L. K., N. Kasahara, and L. Kedes.** 2001. 3PO, a novel nonviral gene delivery system using engineered Ad5 penton proteins. Gene Ther. **8:**797–803.
34. **Medina-Kauwe, L. K., V. Leung, L. Wu, and L. Kedes.** 2000. Assessing the binding and endocytosis activity of cellular receptors using GFP-ligand fusions. BioTechniques **29:**602–604.
35. **Meier, O., K. Boucke, S. V. Hammer, S. Keller, R. P. Stidwill, S. Hemmi, and U. F. Greber.** 2002. Adenovirus triggers macropinocytosis and endosomal leakage together with its clathrin-mediated uptake. J. Cell Biol. **158:**1119–1131.
36. **Meier, O., and U. F. Greber.** 2003. Adenovirus endocytosis. J. Gene Med. **5:**451–462.
37. **Mircheff, A. K.** 1994. Water and electrolyte secretion and fluid modification, p. 466–472. *In* D. M. Albert and F. A. Jacobiec (ed.), Principles and practice of ophthalmology, 2nd ed. Saunders, Philadelphia, Pa.
38. **Mircheff, A. K., C. E. Ingham, R. W. Lambert, K. L. Hales, C. B. Hensley, and S. C. Yiu.** 1987. Na+/H+ antiporter in lacrimal acinar cell basal-lateral membranes. Investig. Ophthalmol. Vis. Sci. **28:**1726–1729.
39. **Pflugfelder, S. C., A. Solomon, and M. E. Stern.** 2000. The diagnosis and management of dry eye: a twenty-five-year review. Cornea **19:**644–649.
40. **Rentsendorj, A., H. Agadjanian, X. Chen, M. Cirivello, M. Macveigh, L. Kedes, S. Hamm-Alvarez, and L. K. Medina-Kauwe.** 2005. The Ad5 fiber mediates nonviral gene transfer in the absence of the whole virus, utilizing a novel cell entry pathway. Gene Ther. **12:**225–237.
41. **Rentsendorj, A., J. Xie, M. Macveigh, H. Agadjanian, S. Bass, D. H. Kim, J. Rossi, S. F. Hamm-Alvarez, and L. K. Medina-Kauwe.** 2006. Typical and atypical trafficking pathways of Ad5 penton base recombinant protein: implications for gene transfer. Gene Ther. **13:**821–836.
42. **Seth, P.** 1994. Adenovirus-dependent release of choline from plasma membrane vesicles at an acidic pH is mediated by the penton base protein. J. Virol. **68:**1204–1206.
43. **Seth, P., D. FitzGerald, H. S. Ginsberg, M. Willingham, and I. Pastan.** 1984. Evidence that the penton base of adenovirus is involved in potentiation of toxicity of Pseudomonas exotoxin conjugated to epidermal growth factor. Mol. Cell. Biol. **4:**1528–1533.
44. **Sharp, P. A.** 2001. RNA interference—2001. Genes Dev. **15:**485–490.
45. **Spillmann, D.** 2001. Heparan sulfate: anchor for viral intruders? Biochimie **83:**811–817.
46. **Swanson, J. A., and C. Watts.** 1995. Macropinocytosis. Trends Cell Biol. **5:**424–428.
47. **Tyagi, M., M. Rusnati, M. Presta, and M. Giacca.** 2001. Internalization of HIV-1 tat requires cell surface heparan sulfate proteoglycans. J. Biol. Chem. **276:**3254–3261.
48. **Wadia, J. S., R. V. Stan, and S. F. Dowdy.** 2004. Transducible TAT-HA fusogenic peptide enhances escape of TAT-fusion proteins after lipid raft macropinocytosis. Nat. Med. **10:**310–315.
49. **Wang, Y., G. Jerdeva, F. A. Yarber, S. R. da Costa, J. Xie, L. Qian, C. M. Rose, C. Mazurek, N. Kasahara, A. K. Mircheff, and S. F. Hamm-Alvarez.** 2003. Cytoplasmic dynein participates in apically targeted stimulated secretory traffic in primary rabbit lacrimal acinar epithelial cells. J. Cell Sci. **116:**2051–2065.
50. **Wang, Y., J. Xie, F. A. Yarber, C. Mazurek, M. D. Trousdale, L. K. Medina-Kauwe, N. Kasahara, and S. F. Hamm-Alvarez.** 2004. Adenoviral capsid modulates secretory compartment organization and function in acinar epithelial cells from rabbit lacrimal acini. Gene Ther. **11:**970–981.
51. **West, M. A., M. S. Bretscher, and C. Watts.** 1989. Distinct endocytotic pathways in epidermal growth factor-stimulated human carcinoma A431 cells. J. Cell Biol. **109:**2731–2739.
52. **Wu, K., G. V. Jerdeva, S. R. da Costa, E. Sou, J. E. Schechter, and S. F. Hamm-Alvarez.** Molecular mechanisms of lacrimal acinar secretory vesicle exocytosis. Exp. Eye Res. **83:**84–96.
53. **Xia, D., L. J. Henry, R. D. Gerard, and J. Deisenhofer.** 1994. Crystal structure of the receptor-binding domain of adenovirus type 5 fiber protein at 1.7 A resolution. Structure **2:**1259–1270.
54. **Xie, J., L. Qian, Y. Wang, S. F. Hamm-Alvarez, and A. K. Mircheff.** 2004. Role of the microtubule cytoskeleton in traffic of EGF through the lacrimal acinar cell endomembrane network. Exp. Eye Res. **78:**1093–1106.
55. **Xie, J., L. Qian, Y. Wang, C. M. Rose, T. Yang, T. Nakamura, S. F. Hamm-Alvarez, and A. K. Mircheff.** 2004. Novel biphasic traffic of endocytosed EGF to recycling and degradative compartments in lacrimal gland acinar cells. J. Cell. Physiol. **199:**108–125.
56. **Yoneda, A., and J. R. Couchman.** 2003. Regulation of cytoskeletal organization by syndecan transmembrane proteoglycans. Matrix Biol. **22:**25–33.
57. **Yoshimura, A.** 1985. Adenovirus-induced leakage of co-endocytosed macromolecules into the cytosol. Cell Struct. Funct. **10:**391–404.
58. **Yoshimura, K., M. A. Rosenfeld, P. Seth, and R. Crystal.** 1993. Adenovirus-mediated augmentation of cell transformation with unmodified plasmid vectors. J. Biol. Chem. **268:**2300–2303.
59. **Zhang, L., S. R. da Costa, F. A. Yarber, M. Runnegar, and S. F. Hamm-Alvarez.** 2000. Protein phosphatase inhibitors alter cellular microtubules and reduce carbachol-dependent protein secretion in lacrimal acini. Curr. Eye Res. **20:**373–383.
60. **Zhang, Y., and J. M. Bergelson.** 2005. Adenovirus receptors. J. Virol. **79:**12125–12131.
61. **Zhu, Z., D. Stevenson, J. E. Schechter, A. K. Mircheff, R. W. Crow, R. Atkinson, T. Ritter, S. Bose, and M. D. Trousdale.** 2003. Tumor necrosis factor inhibitor gene expression suppresses lacrimal gland immunopathology in a rabbit model of autoimmune dacryoadenitis. Cornea **22:**343–351.
62. **Zhu, Z., D. Stevenson, J. E. Schechter, A. K. Mircheff, T. Ritter, L. Labree, and M. D. Trousdale.** 2004. Prophylactic effect of IL-10 gene transfer on induced autoimmune dacryoadenitis. Investig. Ophthalmol. Vis. Sci. **45:**1375–1381.